The white-footed deermouse, an infection-tolerant reservoir for several zoonotic agents, tempers interferon responses to endotoxin in comparison to the mouse and rat

Version 3

Ana Milovic[a], Jonathan V. Duong[a], Alan G. Barbour[b,1]

[a] Department of Microbiology & Molecular Genetics, University of California Irvine
[b] Departments of Medicine, Microbiology & Molecular Genetics, and Ecology & Evolutionary Biology, University of California Irvine
[1] Correspondence: abarbour@uci.edu

ABSTRACT

The white-footed deermouse *Peromyscus leucopus*, a long-lived rodent, is a key reservoir for agents of several zoonoses, including Lyme disease. While persistently infected, this deermouse is without apparent disability or diminished fitness. For a model for inflammation elicited by various pathogens, the endotoxin lipopolysaccharide (LPS) was used to compare genome-wide transcription in blood by *P. leucopus*, *Mus musculus* and *Rattus norvegicus* and adjusted for white cell concentrations. Deermice were distinguished from the mice and rats by LPS response profiles consistent with non-classical monocytes and alternatively-activated macrophages. LPS-treated *P. leucopus*, in contrast to mice and rats, also displayed little transcription of interferon-gamma and lower magnitude fold-changes in type 1 interferon-stimulated genes. This was associated with comparatively reduced transcription of endogenous retrovirus sequences and cytoplasmic pattern recognition receptors in the deermice. The results reveal a mechanism for infection tolerance in this species and perhaps other animal reservoirs for agents of human disease.

Keywords

lipopolysaccharide, innate immunity, interferon-gamma, type 1 interferons, interferon stimulated genes, endogenous retroviruses, pathogen recognition receptors

INTRODUCTION

How does the white-footed deermouse *Peromyscus leucopus* continue to thrive while sustaining infections with disease agents it serves as reservoir for [4]? The diverse tickborne pathogens (and diseases) for humans include the extracellular bacterium *Borreliella burgdorferi* (Lyme disease), the intracellular bacterium *Anaplasma phagocytophilum* (anaplasmosis), the protozoan *Babesia microti* (babesiosis), and the Powassan flavivirus (viral encephalitis). Most deermice remain persistently infected but display scant inflammation in affected tissues [23, 52, 64], and without apparent consequence for fitness [83, 92].

A related question—conceivably with the same answer--is what accounts for the two-to-three fold longer life span for *P. leucopus* than for the house mouse, *Mus musculus* [48, 79]? The abundance of *P. leucopus* across much of North America [34, 66] and its adaptation to a variety of environments, including urban areas and toxic waste sites [11, 50, 67], indicates successful adjustment to changing

landscapes and climate. *Peromyscus* species, including the hantavirus reservoir *P. maniculatus* [65], are more closely related to hamsters and voles in family Cricetidae than to mice and rats of family Muridae [15].

As a species native to North America, *P. leucopus* is an advantageous alternative to the Eurasian-origin house mouse for study of natural variation in populations that are readily accessible [9, 53]. A disadvantage for the study of any *Peromyscus* species is the limited reagents and genetic tools of the sorts that are applied for mouse studies. As an alternative, we study *P. leucopus* with a non-reductionist approach that is comparative in design and agnostic in assumptions [3]. The genome-wide expression comparison for *P. leucopus* is with *M. musculus* and, added here, the brown rat *Rattus norvegicus*. Given the wide range of pathogenic microbes that deermice tolerate, we use the bacterial endotoxin lipopolysaccharide (LPS) as the primary experimental treatment because the inflammation it elicits within a few hours has features common to different kinds of serious infections, not to mention severe burns and critical injuries [96].

We previously reported that a few hours after injection of LPS, *P. leucopus* and *M. musculus* had distinguishing profiles of differentially expressed genes (DEG) in the blood, spleen, and liver [3]. In brief, the inflammation phenotype of deermice was consistent with an "alternatively activated" or M2-type macrophage polarization phenotype instead of the expected "classically activated" or M1-type polarization phenotype that was observed for *M. musculus* [69]. The deermice also differed from mice in displaying evidence of greater neutrophil activation and degranulation after LPS exposure. The potentially damaging action from neutrophil proteases and reactive oxygen species appeared to be mitigated in part in *P. leucopus* by proteins like secretory leukocyte protease inhibitor (Slpi) and superoxide dismutase 2 (Sod2).

Here, we first address whether the heightened transcription of neutrophil-associated genes in *P. leucopus* is attributable to differences in numbers of white cells in the blood. To better match for genetic diversity, we substituted outbred *M. musculus* for the inbred BALB/c mouse of the previous study. We retained the experimental protocol of short-term responses to LPS. This main experiment was supplemented by a study of rats under the similar conditions, by an investigation of a different dose of LPS and duration of exposure in another group of deermice, and by analysis of deermice infected with a bacterium lacking LPS. The focus was on the blood of these animals, not only because the distinctions between species in their transcriptional profiles were nearly as numerous for this specimen as for spleen and liver [3], but also because for ecological and immunological studies of natural populations of *Peromyscus* species blood is obtainable from captured-released animals without their sacrifice.

The results inform future studies of *Peromyscus* species, not only with respect to microbial infections and innate immunity, but conceivably also determinants of longevity and resilience in the face of other stressors, such as toxic substances in the environment. The findings pertain as well to the phenomenon of infection tolerance broadly documented in other reservoirs for human disease agents, such as betacoronaviruses and bats [57]. Less directly, the results provide for insights about maladaptive responses among humans to microbes, from systemic inflammatory response syndrome (SIRS) to post-infection fatigue syndromes.

RESULTS

LPS experiment and hematology studies.

Twenty adult animals each for *P. leucopus* and *M. musculus* and equally divided between sexes received by intraperitoneal injection either purified *E. coli* LPS at a dose of 10 μg per g body mass or saline alone (Table 1). Within 2 h LPS-treated animals of both species displayed piloerection and sickness behavior, i.e. reduced activity, hunched posture, and huddling. By the experiment's termination at 4 h, 8 of 10 *M. musculus* treated with LPS had tachypnea, while only one of ten LPS-treated *P. leucopus* displayed this sign of the sepsis state ($p = 0.005$).

Table 1. Characteristics and treatments of *Mus musculus* CD-1 and *Peromyscus leucopus* LL stock

Animal	Genus	Sex	Age (d)	Mass (g)	Treatment	Tachypnea	Hct * (%)	MCV *	WBC *	Neutrophils	Lymphocytea	Monocytes	Eosinophils	Neutrophil/ Lymphocyte
MM19	*Mus*	female	149	60.4	control	no	71	62	3800	570	2926	190	114	0.19
MM21	*Mus*	female	149	51.4	control	no	51	59	8600	826	4897	177	0	0.17
MM23	*Mus*	female	149	30.6	control	no	51	.	1500	135	1305	60	0	0.10
MM25	*Mus*	female	149	42.1	control	no	65	61	7900	1106	6557	237	0	0.17
MM27	*Mus*	female	149	39.7	control	no	58	62	3700	962	2257	333	148	0.43
MM1	*Mus*	male	149	50.9	control	no	67	59	3300	726	2376	198	0	0.31
MM17	*Mus*	male	149	40.8	control	no	51	.	7000	4970	2030	0	0	2.45
MM3	*Mus*	male	149	45.8	control	no	58	59	4300	344	3655	301	0	0.09
MM5	*Mus*	male	149	41.2	control	no	60	57	5400	810	4266	324	0	0.19
MM7	*Mus*	male	149	44.1	control	no	47	58	3800	798	2736	266	0	0.29
MM31	*Mus*	female	149	65.5	LPS	yes	53	58	1900	209	1539	114	38	0.14
MM33	*Mus*	female	149	48.4	LPS	yes	62	62	3200	256	2784	96	64	0.09
MM35	*Mus*	female	149	40.5	LPS	yes	49	64	2200	528	1518	88	66	0.35
MM37	*Mus*	female	149	38.5	LPS	no	54	65	1900	152	1634	57	57	0.09
MM39	*Mus*	female	149	40.2	LPS	yes	61	63	600	60	510	12	18	0.12
MM11	*Mus*	male	149	57.4	LPS	yes	59	58	2600	572	1898	104	0	0.30
MM13	*Mus*	male	149	58.5	LPS	yes	66	59	3700	1258	2183	259	0	0.58
MM15	*Mus*	male	149	51.0	LPS	yes	33	56	1800	90	1602	90	0	0.06
MM29	*Mus*	male	149	39.1	LPS	no	53	59	1800	306	1368	72	54	0.22
MM9	*Mus*	male	149	44.1	LPS	yes	58	.	1300	260	858	182	0	0.30
24841	*Peromyscus*	female	162	19.9	control	no	58	48	5100	204	4590	102	204	0.04
24842	*Peromyscus*	female	164	18.3	control	no	47	48	3900	663	3003	117	117	0.22
24843	*Peromyscus*	female	162	20.5	control	no	45	46	4200	942	3150	42	84	0.30
24845	*Peromyscus*	female	161	18.7	control	no	49	48	9100	2002	6916	182	0	0.29
24853	*Peromyscus*	female	160	22.8	control	no	42	.	4800	1008	2880	864	1	0.35
24852	*Peromyscus*	male	162	19.4	control	no	44	46	7100	994	4970	284	852	0.20
24861	*Peromyscus*	male	157	20.8	control	no	28	50	1300	104	1053	91	52	0.10
24863	*Peromyscus*	male	157	17.1	control	no	26	58	7200	720	5904	288	288	0.12
24869	*Peromyscus*	male	143	29.0	control	no	48	52	6000	1260	4260	180	240	0.30
24876	*Peromyscus*	male	142	16.1	control	no	54	48	9700	2716	6208	194	485	0.44
24846	*Peromyscus*	female	162	22.7	LPS	no	23	47	1100	231	718	44	44	0.32
24847	*Peromyscus*	female	162	16.7	LPS	no	39	.	1500	570	675	180	75	0.84
24848	*Peromyscus*	female	166	16.2	LPS	no	43	49	2700	918	1701	27	54	0.54
24850	*Peromyscus*	female	157	19.4	LPS	no	46	.	3300	1551	1683	66	0	0.92
24851	*Peromyscus*	female	161	25.4	LPS	no	24	47	2300	552	1242	437	69	0.44
24855	*Peromyscus*	male	165	27.1	LPS	no	51	51	2100	1281	714	42	63	1.79
24860	*Peromyscus*	male	160	17.8	LPS	yes	42	54	13200	6996	3696	1320	1056	1.89
24865	*Peromyscus*	male	160	16.7	LPS	no	49	46	1800	396	1080	288	0	0.37
24873	*Peromyscus*	male	145	23.2	LPS	no	43	48	2200	550	1430	110	110	0.38
24879	*Peromyscus*	male	145	22.0	LPS	no	40	.	1100	220	538	352	0	0.41

* Abbreviations: Hct, hematocrit; MCV, mean cellular volume of erythrocytes; WBC, white blood cell count

Table 1. Characteristics (including hematology values) and treatments (with or without LPS) of *Mus musculus* CD-1 and *Peromyscus leucopus* LL stock

Within a given species there was little difference between LPS-treated and control animals in values for erythrocytes. But overall the deermice had lower mean (95% confidence interval) hematocrit at 42 (36-48)%, hemoglobin concentration at 13.8 g/dL (12.1-15.5), and mean corpuscular volume for erythrocytes at 49 fL (47-51) than *M. musculus* with respective values of 56 (51-62)%, 16.1 g/dL (14.6-17.7), and 60 fL (58-62) ($p < 0.01$). These hematology values for adult CD-1 *M. musculus* and LL stock *P. leucopus* in this study were close to what had been reported for these colony populations [18, 94].

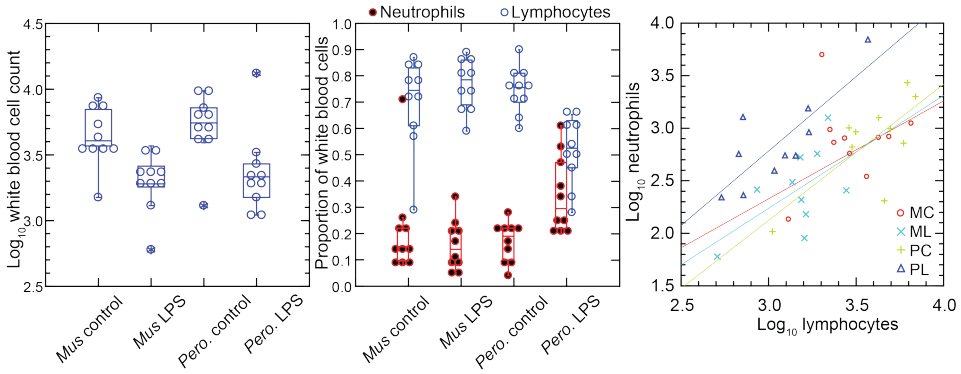

Figure 1. Total white blood cells, neutrophils, and lymphocytes of *Mus musculus* (M) and *Peromyscus leucopus* (P) with or without (control; C) treatment with 10 µg lipopolysaccharide (LPS; L) per g body mass 4 h previous. The box plots of left and center panels show values of individual animals and compiled median, quartiles, and extreme values. The linear regressions of the right panel are color-coded according to the species and treatment designations. The outlier value for a *M. musculus* control (MM17) was excluded from the linear regression for that group.

In contrast to red blood cells, the mean numbers of white blood cells in the LPS groups in both species were lower than those of control groups (Figure 1). Controls had a mean 4.9 (3.5-6.4) x 10^3 white cells per µl among *M. musculus* and 5.8 (4.2-7.4) x 10^3 white cells per µl among *P. leucopus* (p = 0.41). For the LPS-treated animals the values were 2.1 (1.5-2.7) x 10^3 for mice and 3.1 (0.9-5.4) x 10^3 for deermice (p = 0.39). However, there was difference between species among LPS-treated animals in the proportions of neutrophils and lymphocytes in the white cell population. The ratios of neutrophils to lymphocytes were 0.25 (0.14-0.45) and 0.20 (0.13-0.31) for control *M. musculus* and *P. leucopus*, respectively (p = 0.53). But under the LPS condition. the neutrophil-to-lymphocyte ratio was 0.18 (0.11-0.28) for mice and 0.64 (0.42-0.97) for deermice (p = 0.0006). The regression curves for plots of neutrophils and lymphocytes for LPS-treated and control *P. leucopus* and LPS-treated *M. musculus* had similar slopes, but the y-intercept was shifted upwards towards a higher ratio of neutrophils to lymphocytes for blood from the LPS group of deermice. Control group mice and deermice and LPS-treated mice had similar percentages (~5%) of monocytes in their blood; the mean monocyte percentage rose to 10% in LPS treated deermice (p = 0.12). Eosinophil percentages tended to be higher in deermice at a mean 3.4 (2.1-4.7)% than mice at 1.2 (0.5-1.9)% under either condition (p = 0.004).

In the *P. leucopus* experiment with a 10-fold lower dose of LPS and a 12 hour duration, the mean (95% confidence interval) white blood cell count (x 10^3) at termination 3.5 (2.5-4.5) in controls and 7.9 (6.0-9.7) in the LPS-treated (p = 0.01). Even with the higher overall white blood cell count the increase white cells was proportionately higher for neutrophils than for lymphocytes, as was seen in the deermice in the higher dose LPS experiment. The ratio of neutrophils-to-lymphocytes was 0.20 (0.07-0.32) in the controls and 0.38 (0.26-0.50) in the LPS-treated (p = 0.10).

The higher neutrophil to lymphocyte ratio in the deermice exposed to LPS was consistent with the greater neutrophil activation noted by transcriptional analysis [3]. But many individual genes that constitute this and related gene ontology (GO) terms had transcription levels in the deermice that far exceeded a three-fold difference in neutrophil counts. For some genes the differences were a hundred or more fold, which suggested that the distinctive LPS transcriptional response profile between species was not attributable solely to neutrophil counts.

Genome-wide expression in blood of deermice and mice

We used the respective transcript sets from the reference genomes for *P. leucopus* and *M. musculus* for deep coverage RNA-seq with paired-end ~150 nt reads (Dryad Tables D1 and D2). Principle component analyses (PCA) of the *P. leucopus* data and *M. musculus* data revealed that untreated controls had coherent profiles within each species (Figure 2). With the exception of one mouse, the LPS-treated *M. musculus* were also in a tight PCA cluster. In contrast, the LPS-treated deermice displayed a diversity of genome-wide transcription profiles and limited clustering.

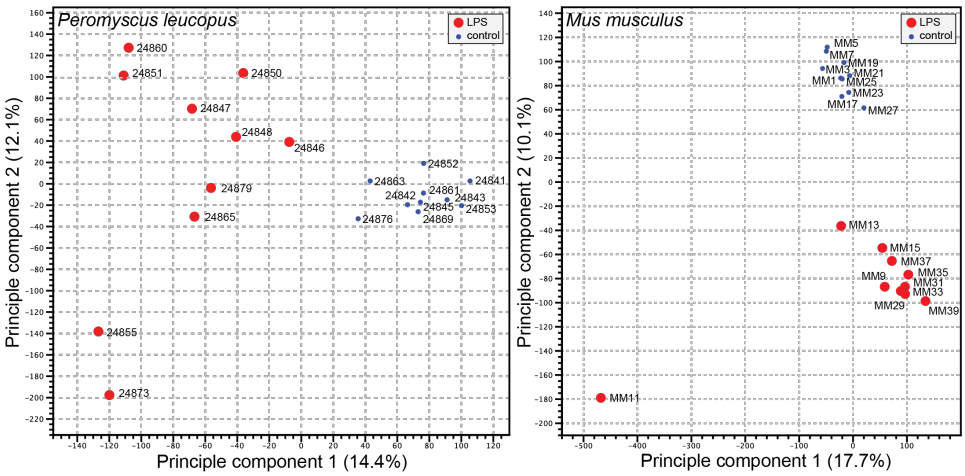

Figure 2. Principle component analysis of genome-wide RNA-seq data of *P. leucopus* or *M. musculus* with or without (blue dot) treatment with LPS 4 h previous. The individual animals listed in Table 1 are indicated on the graphs. The insets indicate the size and color of the symbol for the experimental condition (LPS-treated or control).

For both species the number of genes with higher expression with LPS exposure exceeded those with lower or unchanged expression (Dryad Tables D3 and D4). For *P. leucopus* and *M. musculus* the mean fold-changes were 1.32 (1.29-1.35) and 1.30 (1.24-1.36), respectively (p = 0.31). For GO term analysis the absolute fold-change criterion was ≥ 2. Because of the ~3-fold greater number of transcripts for the *M. musculus* reference set than the *P. leucopus* reference set, application of the same false-discovery rate (FDR) threshold for both datasets would favor the labeling of transcripts as DEGs in *P. leucopus*. Accordingly, the FDR p values were arbitrarily set at $<5 \times 10^{-5}$ for *P. leucopus* and $<3 \times 10^{-3}$ for *M. musculus* to provide approximately the same number of DEGs for *P. leucopus* (1154 DEGs) and *M. musculus* (1266 DEGs) for the GO term comparison.

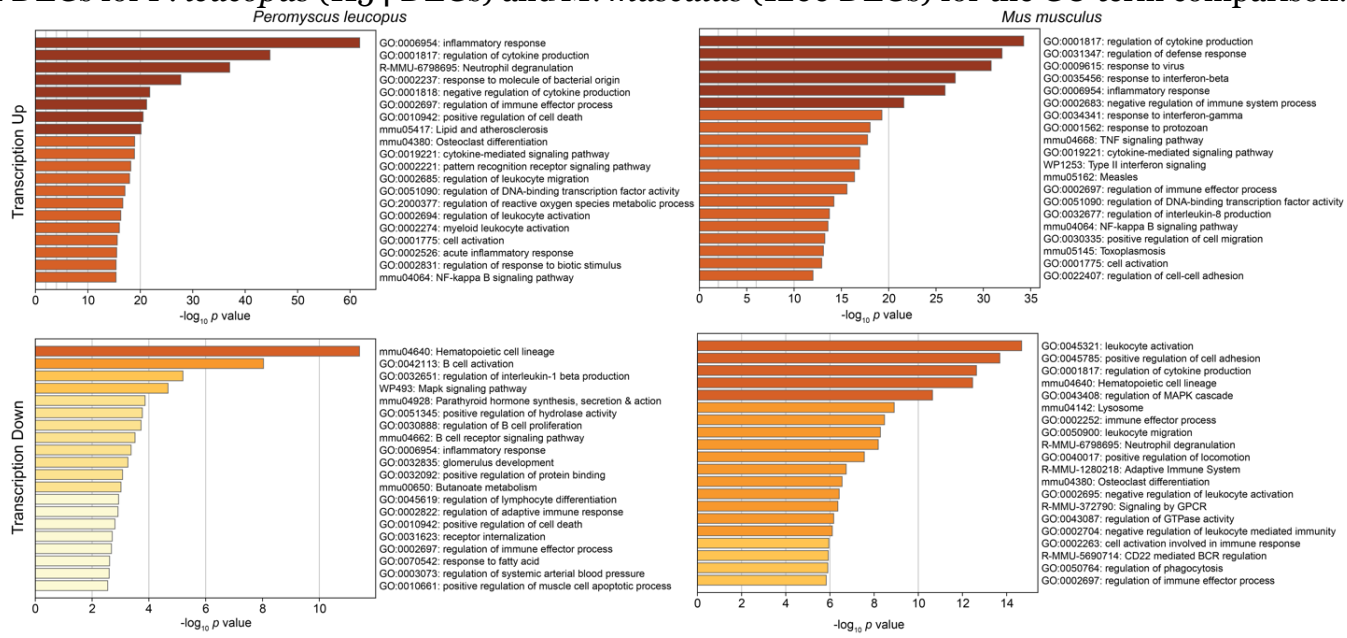

Figure 3. Gene Ontology (GO) term clusters associated with up-regulated genes (upper panels) and down-regulated genes (lower panels) of *P. leucopus* (left panels) and *M. musculus* (right panels) treated with LPS in comparison with untreated controls of each species. The scale for the *x*-axes for the panels was determined by the highest $-\log_{10}$ p values in each of the 4 sets. The horizontal bar color, which ranges from white to dark brown through shades of yellow through orange in between, is a schematic representation of the $-\log_{10}$ p values.

Figure 3 shows the GO terms for the top 20 clusters by ascending p-value for up-regulated and down-regulated in *P. leucopus* and the corresponding categories for *M. musculus*. The up-regulated gene profile for *P. leucopus* featured terms associated with "neutrophil degranulation", "myeloid leukocyte activation", "leukocyte migration", and "response to molecule of bacterial origin". Other sets of up-regulated genes for the deermice were "negative regulation of cytokine production" and "regulation of reactive oxygen species metabolic process". None of these were among the top 20 up-regulated clusters for *M. musculus*. Indeed, "leukocyte activation" and "leukocyte migration" were GO terms for down-regulated DEGs in *M. musculus*. Distinctive GO terms for up-regulated genes distinguishing mice from deermice were "response to virus", "response to interferon-beta", "response to interferon-gamma", "response to protozoan", and "type II interferon signaling".

By arbitrary criterion of 100 for the top DEGs by ascending p value for each species, 24 genes were shared between species (Supplementary Materials Table S1). These included up-regulated Bcl3, Ccl3, Cxcl1, Cxcl2, Cxcl3, Cxcl10, Il1rn, and Sod2. Among the 100 mouse DEGs, 20 were constituents of GO terms "response to virus" or "response to interferon-beta" and only 3 were members of GO term sets "response to molecule of bacterial origin" or "response to lipopolysaccharide". In contrast,

among the top 100 deermouse DEGs, there were only 2 associated with the virus or type 1 interferon GO terms, but 12 were associated with either or both of the bacterial molecule GO terms.

We confirmed the sex identification for each sample with sex-specific transcripts of Xist for females and Ddx3y for males [3]. For female and male *P. leucopus* there were 5012 transcripts out of 54,466 in the reference set for which there were TPM values of ≥10 in at least one animal in each of the sexes under either condition (Dryad Table D5). The comparison of females to males by fold-changes between LPS-treated and control animals revealed transcripts that were differentially expressed between sexes under LPS treatment (Table S2 and Figure 4). Some were down-regulated in one sex while unchanged in expression in the opposite sex. Of note in this category were different isoforms or variants of Lilra6 (leukocyte immunoglobulin-like receptor, subfamily A, member 6), one of a family of orphan receptors of myeloid cells [8]. The opposite case was exemplified by the Dnajc15 and Hspa8 genes for two chaperones: DnaJ heat shock protein family (Hsp40) member C15 and heat shock protein 8, respectively. These were substantially lower in transcription in the LPS-treated females than in untreated animals, but little changed in LPS-treated males. Coordinates for some other genes, e.g. Saa5 and Cxcl2, fell outside the prediction limits at the extreme end of up-regulation, but their vectors were within 20-25° of each other. While these and other sex-associated differences merit attention for future studies, overall they were not of sufficient number or magnitude in our view to warrant division by sex for the subsequent analyses, which had the aim of identifying differences applicable for both females and males.

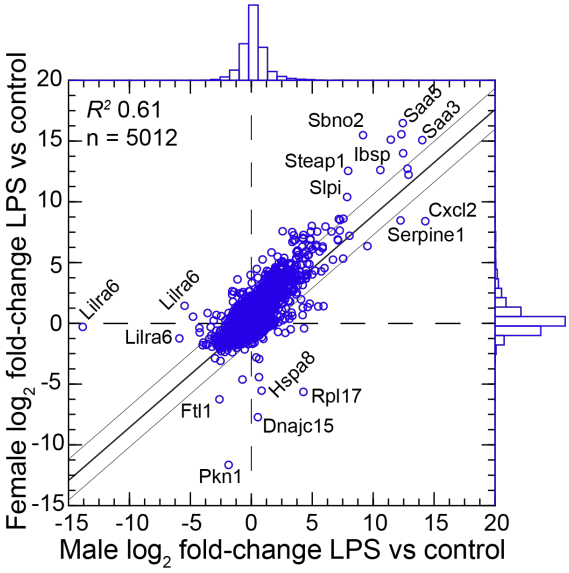

Figure 4. Scatter plot with linear regression of pairs of $\log_2$-transformed mean fold-changes between LPS-treated and control *P. leucopus* by male and female sex. The 5012 reference transcripts from the genome reference set are defined in the text and listed in Table S2 and Dryad Table D5. The coefficient of determination (R^2), the 95% upper and lower prediction limits for the regression line, and distributions of the values on the *x*- and *y*-axes are shown. Selected genes for which their *x*-*y* coordinates fall outside the limits of prediction are labeled. Cxcl2, Ibsp, Saa3, Saa5, Sbno2, Serpine1, Slpi, and Steap1 were noted as up-regulated DEGs for the groups with both sexes (Table S1).

Targeted RNA seq analysis

The emerging picture was of *P. leucopus* generally responding to LPS exposure as if infected with an extracellular bacterial pathogen, including with activated neutrophils. While *M. musculus* animals of both sexes shared with *P. leucopus* some features of an antibacterial response, they also displayed type 1 and type 2 interferon type response profiles associated with infections with viruses and intracellular bacteria and parasites.

Going forward, the challenge for a cross-species RNA-seq was commensurability between annotated transcripts of reference sets. Orthologous genes can be identified, but mRNA isoforms and their 5' and 3' untranslated regions may not fully correspond. Accordingly, we limited targeted

RNA-seq to protein coding sequences of mRNAs for the corresponding sets of *P. leucopus* and *M. musculus* sequences.

The 113 mRNA coding sequences, which are listed in Methods, were drawn from the identified DEGs for *P. leucopus* and *M. musculus* from the genome-wide RNA-seq. For cross-species normalization we first evaluated three methods: (1) normalization using the ratio of mean total reads for all samples to total reads for a given sample, (2) the ratio of reads mapping to a given target gene (i.e. the numerator) to the reads to the mitochondrial 12S rRNA gene (i.e. the denominator), or (3) when the denominator instead was the myeloid cell marker CD45 (protein tyrosine phosphatase, receptor type C) encoded by the Ptprc gene. In humans, mice, and hamsters, Ptprc is expressed by nucleated hematopoietic cells, and CD45 is commonly used as a white cell marker for flow cytometry [82]. The coefficients of determination (R^2) between comparison pairs (e.g. normalized total reads vs. Ptprc ratio) within a species were ≥ 0.95 (Supplementary Materials Figure S1 and Table S3). There was also little difference between the choice of Ptprc or 12S rRNA transcripts as denominator with respect to cross-species comparisons of LPS-treated to control fold changes. Given the widespread adoption of CD45 for flow cytometry, we chose Ptprc as denominator and as an adjustment for white cell numbers in the samples. Pearson correlation between log-transformed total white blood cell counts and normalized reads for Ptprc across 40 animals representing both species, sexes, and treatments was 0.40 (p = 0.01).

Figure 5 comprises plots of the log-transformed mean ratios for the 10 *P. leucopus* controls and 10 *M. musculus* controls and for the 10 *P. leucopus* and 10 *M. musculus* treated with LPS (Table S4). For untreated animals (left panel) there was high correlation and a regression coefficient of ~1 between the paired data for deermice and mice. The mitochondrial cytochrome oxidase 1 gene (MT-Co1) and S100a9, a subunit of calprotectin, were comparably transcribed. But, there were other coding sequences that stood out for either their greater or lesser transcription in untreated deermice than mice. Two examples of greater expression were Arg1 and MX dynaminin-like GTPase 2 (Mx2), an ISG, while two examples of lesser expression were matrix metalloprotease 8 (Mmp8) and Slpi. There was low to undetectable transcription of Nos2 and interferon-gamma (Ifng) in the blood of controls of both species.

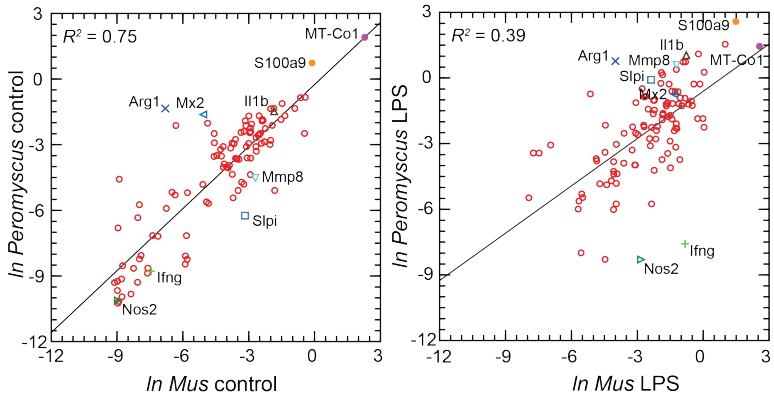

Figure 5. Scatter plots with linear regression of pairs of log-transformed (*ln*) normalized RNA-seq reads for selected coding sequences for control *P. leucopus* and *M. musculus* (left panel) and LPS-treated *P. leucopus* and *M. musculus* (right panel). The R^2 values and selected genes (each with a different symbol) are indicated in each graph.

For the LPS-treated animals (right panel Figure 5) there was, as expected for this selected set, higher expression of the majority genes and greater heterogeneity among *P. leucopus* and *M. musculus* animals in their responses for represented genes. In contrast to the findings with controls, Ifng and Nos2 had higher transcription in treated mice. In deermice the magnitude of difference in the transcription between controls and LPS-treated was less. A comparatively restrained transcriptional response in deermice was also noted for Mx2. On the other hand, there were greater fold-change from baseline in *P. leucopus* than in *M. musculus* for interleukin-1 beta (Il1b), Mmp8, Slpi, and S100a9.

Table 2 lists all the selected targets with the means and confidence intervals for the normalized values for controls and LPS-treated *M. musculus* and controls and LPS-treated *P. leucopus* (Table S4). Box plots for a selected 54 of these targets organized by functional characteristics are provided in Figure S2. The fold-changes within each species and between treatments across species are given. The final column is the ratio of the fold-change between LPS to control in *P. leucopus* to the corresponding value for *M. musculus*. This along with the derived heat-map of these ratios, presented in the second column, indicates the genes for which there was little difference between species in their responses to LPS--either up or down--as well as those that were comparatively greater or lesser in one species or the other. Several of these genes are considered in other specific contexts below. Of note here are the places of Nos2 and Ifng at the bottom of the table, and Il1b near the top at position 20.

Table 2. Targeted RNA-seq of blood of *Peromyscus leucopus* and *Mus musculus* 4 hours after intraperitoneal injection of lipopolysaccharide (LPS) or saline control

Gene *	Heatmap †	Mus control mean (95% CI) ‡	Mus LPS mean (95% CI)	Mus FC LPS vs control**	Mus FDR p value**	Peromyscus control mean (95% CI)	Peromyscus LPS mean (95% CI)	Peromyscus FC LPS v control	Peromyscus FDR p value	Peromyscus v Mus control FC	Peromyscus v Mus LPS FC	Peromyscus v Mus LPS/control †
Ibsp		0.51 (0.28-0.93)	5.99 (2.04-17.6)	11.7	2E-03	0.17 (0.06-0.47)	471 (305-728)	2720	3E-10	0.34	78.6	233
Slpi		42.0 (32.6-54.0)	93.2 (44.5-195)	2.22	7E-02	1.94 (0.96-3.94)	921 (636-1333)	474	1E-10	0.05	9.88	213
Steap1		0.13 (0.10-0.16)	0.58 (0.21-1.60)	4.52	1E-02	0.09 (0.05-0.17)	31.7 (16.3-61.4)	335	1E-09	0.73	54.3	74.2
Saa3		2.82 (0.89-8.95)	458 (165-1267)	162	7E-06	0.21 (0.12-0.37)	2052 (1273-3306)	9934	2E-13	0.07	4.48	61.2
Lpo		0.13 (0.09-0.20)	0.37 (0.19-0.72)	2.78	2E-02	0.03 (0.03-0.04)	4.10 (1.44-11.7)	118	1E-07	0.26	11.2	42.4
Mmp8		67.4 (34.3-133)	298 (187-477)	4.43	3E-03	10.9 (4.26-27.8)	1823 (1311-2534)	168	3E-08	0.16	6.11	37.9
Lrg		40.8 (22.1-75.3)	107 (52.2-219)	2.62	7E-02	8.01 (2.98-21.5)	353 (268-464)	44.1	2E-06	0.20	3.30	16.8
Mmp9		222 (147-335)	153 (90.1-258)	0.69	3E-01	154 (96.8-245)	1258 (903-1753)	8.17	2E-06	0.69	8.25	11.9
Csf3		0.14 (0.10-0.19)	7.85 (3.07-20.1)	57.1	6E-07	0.04 (0.03-0.05)	24.5 (8.95-67.1)	648	2E-09	0.27	3.12	11.4
Serpine1		0.51 (0.27-0.93)	11.7 (3.04-45.2)	23.2	9E-04	0.14 (0.06-0.32)	32.8 (4.82-223)	239	9E-05	0.27	2.80	10.3
Fpr2		36.9 (25.8-52.7)	246 (168-362)	6.68	2E-06	8.74 (6.48-11.8)	535 (399-717)	61.2	5E-12	0.24	2.17	9.16
Cxcl3		0.32 (0.17-0.59)	19.6 (12.3-31.3)	60.8	2E-08	0.09 (0.04-0.21)	47.2 (15.9-140)	523	2E-07	0.28	2.41	8.59
Retn		0.35 (0.18-0.68)	0.45 (0.26-0.77)	1.28	6E-01	3.13 (1.80-5.46)	31.8 (22.0-45.9)	10.1	4E-06	8.96	71.1	7.93
Csf3r/Cd114		669 (455-982)	302 (221-411)	0.45	7E-03	423 (318-563)	1445 (1024-2040)	3.42	6E-05	0.63	4.79	7.58
Fcgr3/Cd16		45.7 (31.7-65.8)	70.1 (35.1-140)	1.53	3E-01	44.7 (34.1-58.6)	409 (338-497)	9.17	1E-09	0.98	5.84	5.97
Ptx		0.24 (0.17-0.33)	4.06 (0.94-17.6)	17.0	2E-03	0.05 (0.03-0.09)	4.88 (1.10-21.6)	92.2	4E-05	0.22	1.20	5.42
Fcgr2a		78.8 (59.1-105)	149 (93.8-237)	1.89	4E-02	75.0 (62.0-90.8)	766 (597-983)	10.2	2E-10	0.95	5.14	5.40
Cd177		25.0 (11.1-56.1)	158 (80.2-310)	6.31	4E-03	4.29 (2.12-8.69)	144 (107-194)	33.5	1E-07	0.17	0.91	5.31
Ncf4		134 (112-160)	204 (172-242)	1.52	5E-03	49.1 (38.4-62.9)	317 (258-389)	6.46	5E-09	0.37	1.55	4.24
Il1b		158 (102-244)	464 (341-631)	2.94	1E-03	230 (146-362)	2845 (1998-4052)	12.4	2E-07	1.45	6.14	4.22
Fcgr2b		32.7 (27.4-39.0)	111 (78.2-156)	3.38	1E-05	24.9 (22.4-27.8)	352 (302-409)	14.1	2E-14	0.76	3.18	4.17
Hk3		35.8 (25.7-50.0)	63.6 (46.6-86.8)	1.78	3E-02	85.5 (66.8-109)	602 (468-773)	7.04	1E-08	2.39	9.46	3.96
Fgr		138 (110-174)	161 (125-207)	1.17	4E-01	251 (205-308)	1131 (987-1295)	4.50	3E-09	1.82	7.02	3.85
Tlr4		11.9 (8.62-16.4)	11.9 (6.23-22.8)	1.00	1E+00	29.7 (22.9-38.6)	113 (90.7-141)	3.81	1E-06	2.50	9.49	3.80
Glrx		54.8 (43.1-69.7)	122 (65.4-227)	2.22	4E-02	12.4 (11.1-13.9)	88.4 (71.6-109)	7.11	5E-11	0.23	0.73	3.20
Slc11a1/Nramp		54.9 (41.6-72.5)	75.3 (60.0-94.6)	1.37	1E-01	104 (88.0-123)	424 (308-582)	4.07	1E-06	1.89	5.62	2.97
Ccl3		3.07 (2.20-4.30)	227 (161-320)	73.9	2E-11	0.26 (0.14-0.48)	54.6 (33.2-89.8)	213	1E-09	0.08	0.24	2.88
Tlr1		71.8 (63.3-81.5)	52.2 (37.4-72.8)	0.73	1E-01	36.0 (29.8-43.4)	73.3 (61.6-87.1)	2.04	5E-05	0.50	1.40	2.81
Hmox1		16.0 (12.5-20.6)	27.8 (13.7-56.7)	1.74	2E-01	17.4 (14.9-20.4)	78.2 (51.5-119)	4.49	6E-06	1.09	2.81	2.58
Tnfrsf1a		70.8 (57.2-87.7)	69.3 (45.5-106)	0.98	9E-01	44.6 (34.1-58.4)	105 (89.0-123)	2.34	6E-05	0.63	1.51	2.40
Olfm4		7.41 (3.43-16.0)	162 (98.8-266)	21.9	6E-06	3.56 (1.96-6.44)	181 (101-326)	51.0	1E-07	0.48	1.12	2.33
Sod2		58.1 (48.3-69.9)	412 (262-650)	7.10	8E-07	124 (80.5-192)	2030 (1666-2475)	16.3	5E-09	2.14	4.92	2.30
Il2ra/Cd25		12.3 (3.95-38.3)	8.23 (3.06-22.2)	0.67	6E-01	4.33 (3.80-4.94)	5.77 (4.38-7.61)	1.33	9E-02	0.35	0.70	1.99
Lcn2		29.6 (14.9-58.9)	2797 (1832-4271)	94.5	1E-08	25.2 (11.4-55.9)	4571 (3268-6393)	181	3E-09	0.85	1.63	1.92
Sting		51.2 (42.7-61.3)	47.8 (38.5-59.3)	0.93	7E-01	181 (160-204)	317 (277-363)	1.76	2E-05	3.53	6.64	1.88
Jak2		166 (150-185)	355 (267-472)	2.13	2E-04	6.02 (5.43-6.66)	23.4 (16.5-33.2)	3.89	2E-06	0.04	0.07	1.82
Lmk2		93.9 (82.2-107)	83.5 (66.1-105)	0.89	4E-01	153 (125-188)	236 (163-340)	1.54	6E-02	1.63	2.82	1.73
Il1rn		18.6 (12.1-28.6)	325 (185-572)	17.5	7E-07	17.4 (13.0-23.3)	523 (408-670)	30.0	2E-11	0.94	1.61	1.72
Csf1		8.18 (5.53-12.1)	17.5 (12.0-25.5)	2.14	2E-02	3.32 (2.43-4.55)	12.1 (8.04-18.1)	3.63	1E-04	0.41	0.69	1.70
Cfb		6.28 (4.26-9.25)	111 (46.0-269)	17.7	2E-05	7.93 (3.52-17.9)	225 (140-362)	28.4	3E-06	1.26	2.03	1.60
Itgam/Cd11b		265 (207-339)	361 (283-461)	1.37	1E-01	183 (135-250)	396 (278-564)	2.16	5E-03	0.69	1.10	1.58
Timp1		108 (94.0-124)	192 (117-316)	1.78	5E-02	102 (91.0-114)	272 (226-326)	2.67	1E-07	0.94	1.41	1.50
Socs3		19.9 (12.8-30.8)	254 (213-304)	12.8	2E-08	16.8 (12.1-23.4)	304 (224-413)	18.1	1E-09	0.84	1.20	1.42
Il6		0.27 (0.17-0.42)	9.27 (5.27-16.3)	34.5	5E-08	0.17 (0.09-0.33)	7.77 (1.74-34.6)	45.5	3E-04	0.64	0.84	1.32
Ltf		10.5 (5.82-18.8)	824 (445-1526)	78.8	3E-08	28.5 (12.0-68.0)	2930 (2069-4151)	103	5E-08	2.73	3.56	1.30
S100a9		912 (539-1543)	4540 (2426-8497)	4.98	2E-03	2036 (1240-3344)	12972 (10079-16695)	6.37	6E-06	2.23	2.86	1.28
Cxcl1		0.13 (0.09-0.19)	20.3 (9.03-45.7)	158	9E-09	0.06 (0.03-0.13)	12.3 (3.08-49.0)	198	6E-06	0.48	0.60	1.25
Il10		0.11 (0.10-0.13)	3.57 (1.86-6.87)	31.7	3E-08	0.09 (0.05-0.15)	3.53 (1.13-11.0)	39.6	3E-05	0.79	0.99	1.25
Gapdh		646 (591-707)	1014 (558-1845)	1.57	2E-01	667 (590-754)	1295 (923-1818)	1.94	2E-03	1.03	1.28	1.24
Csf1r/Cd115		233 (201-270)	47.3 (31.7-70.7)	0.20	2E-06	320 (262-390)	78.3 (44.7-137)	0.24	2E-04	1.37	1.66	1.21
Nfkb1		149 (133-168)	336 (283-399)	2.25	1E-06	118 (114-122)	300 (209-431)	2.54	1E-04	0.79	0.89	1.13
Nr3c1		124 (105-148)	119 (101-139)	0.95	7E-01	47.0 (41.5-53.1)	49.9 (38.3-65.2)	1.06	7E-01	0.38	0.42	1.11
Akt1		98.1 (82.8-116)	68.1 (54.1-85.7)	0.69	3E-02	148 (133-164)	113 (88.8-144)	0.76	6E-02	1.51	1.66	1.10
Pkm		538 (469-618)	884 (506-1544)	1.64	1E-01	417 (364-479)	741 (558-983)	1.77	2E-03	0.78	0.84	1.08
Il4ra/Cd124		91.2 (80.2-104)	247 (198-309)	2.71	1E-06	51.7 (47.2-56.7)	150 (122-184)	2.90	8E-08	0.57	0.61	1.07
Fcer2		104 (70.7-153)	15.7 (10.0-24.5)	0.15	1E-05	55.7 (47.6-65.1)	8.93 (4.96-16.1)	0.16	2E-05	0.54	0.57	1.06
Camp		3.12 (1.76-5.54)	285 (145-558)	91.2	3E-08	5.42 (2.26-13.0)	524 (354-776)	96.7	8E-08	1.74	1.84	1.06
Hif1a		53.4 (46.5-61.5)	191 (144-254)	3.58	8E-07	83.6 (77.0-90.8)	299 (203-440)	3.58	1E-05	1.56	1.57	1.00
Padi4		15.9 (8.70-29.0)	41.2 (22.3-76.0)	2.59	5E-02	44.6 (34.1-58.4)	105 (89.0-123)	2.34	6E-05	2.81	2.54	0.90
Bcl3		21.1 (14.8-30.0)	209 (168-260)	9.92	1E-08	18.9 (15.1-23.8)	167 (127-219)	8.80	3E-09	0.90	0.80	0.89
Mt2		0.38 (0.19-0.77)	89.1 (33.8-235)	235	1E-07	0.31 (0.13-0.75)	61.2 (20.5-182)	199	2E-06	0.81	0.69	0.84
Myd88		50.8 (39.5-65.4)	127 (96.0-168)	2.50	2E-04	51.5 (46.6-56.8)	108 (99.7-116)	2.09	5E-09	1.01	0.85	0.84
Thy1		35.0 (22.6-54.2)	25.2 (13.3-48.0)	0.72	5E-01	503 (457-553)	297 (240-368)	0.59	4E-04	14.4	11.8	0.82
Jun		31.4 (23.9-41.2)	157 (105-234)	5.01	6E-06	6.02 (5.43-6.66)	23.4 (16.5-33.2)	3.89	2E-06	0.19	0.15	0.78
Icam		24.1 (20.3-28.6)	301 (257-352)	12.5	3E-12	12.6 (10.5-15.0)	121 (67.3-217)	9.61	2E-06	0.52	0.40	0.77
Cx3cr1		27.9 (21.8-35.7)	3.46 (1.99-6.00)	0.12	4E-06	26.1 (19.0-35.9)	2.45 (1.44-4.15)	0.09	1E-06	0.94	0.71	0.76
Cxcl2		0.16 (0.09-0.26)	119 (76.0-186)	762	6E-12	0.10 (0.04-0.26)	60.2 (19.6-185)	574	2E-07	0.67	0.51	0.75
Akt2		138 (117-163)	275 (182-415)	1.99	9E-03	59.4 (57.1-61.7)	87.6 (71.5-107)	1.47	2E-03	0.43	0.32	0.74
Jak1		415 (386-447)	623 (467-830)	1.50	2E-02	256 (232-281)	277 (214-359)	1.09	6E-01	0.61	0.45	0.72
ERV Gag-pol		3210 (2406-4283)	13633 (10083-18433)	4.3	4E-06	233 (195-278)	692 (548-873)	2.97	2E-06	0.07	0.05	0.70
Pbib		93.7 (82.3-107)	97.2 (58.5-161)	1.04	9E-01	143 (134-153)	102 (71.2-147)	0.71	9E-02	1.53	1.05	0.69
Nox1		0.14 (0.11-0.18)	0.98 (0.65-1.48)	7.01	8E-07	10.1 (8.12-12.5)	45.6 (34.4-60.5)	4.53	3E-07	71.8	46.4	0.65
Tnf		2.99 (2.26-3.96)	19.5 (14.0-27.1)	6.52	3E-07	0.76 (0.42-1.40)	3.10 (1.62-5.95)	4.06	7E-03	0.26	0.16	0.62
Tlr2		26.1 (18.1-37.5)	165 (126-215)	6.31	6E-07	50.8 (37.2-69.5)	194 (128-294)	3.83	1E-04	1.95	1.18	0.61
Cd8		23.8 (19.6-29.0)	17.3 (13.6-22.1)	0.73	7E-02	52.6 (41.6-66.5)	21.3 (10.2-44.7)	0.41	4E-02	2.21	1.23	0.56
Stat1		160 (132-193)	449 (247-814)	2.81	6E-03	256 (221-297)	387 (323-465)	1.51	3E-03	1.60	0.86	0.54
Mapk1		71.1 (65.5-77.0)	92.6 (65.0-132)	1.30	2E-01	67.5 (63.9-71.3)	44.2 (37.4-52.3)	0.65	2E-04	0.95	0.48	0.50
Arg1		1.12 (0.36-3.42)	18.4 (5.99-56.7)	16.5	4E-03	261 (154-441)	2161 (1709-2732)	8.28	2E-06	234	117	0.50
Ccl2		0.16 (0.10-0.27)	12.7 (4.87-33.0)	77.7	8E-07	0.19 (0.07-0.50)	7.42 (3.23-17.0)	38.5	3E-05	1.18	0.58	0.50
Rigi/Ddx58		47.3 (41.9-53.3)	293 (175-491)	6.20	0.00	26.6 (20.5-34.4)	98.9 (76.9-127)	3.72	0.00	0.60	0.29	0.49
MT-Co1		10015 (7976-12576)	13316 (6322-28047)	1.33	5E-01	6608 (4976-8775)	4164 (2563-6765)	0.63	1E-01	0.66	0.31	0.47
Cd4		55.6 (45.7-67.6)	27.5 (19.6-38.8)	0.50	4E-03	88.5 (75.5-104)	19.9 (10.4-38.3)	0.23	5E-04	1.59	0.72	0.45
Socs1		0.82 (0.59-1.13)	45.4 (25.6-80.4)	55.6	3E-09	0.74 (0.53-1.04)	18.4 (9.19-36.9)	24.8	5E-07	0.91	0.41	0.45
Cd3d		81.9 (71.8-93.4)	46.7 (32.8-66.5)	0.57	1E-02	77.1 (64.1-92.7)	18.3 (8.91-37.6)	0.24	2E-03	0.94	0.39	0.42
Mfor		27.9 (24.3-31.9)	40.2 (34.9-46.3)	1.44	2E-03	62.1 (55.6-69.4)	36.3 (27.4-48.1)	0.58	3E-03	2.23	0.90	0.41
Il18		1.78 (1.18-2.70)	4.24 (2.84-6.32)	2.38	1E-02	4.89 (4.22-5.67)	4.15 (2.40-7.18)	0.85	6E-01	2.74	0.98	0.36
Stat2		41.0 (36.6-45.9)	229 (144-364)	5.59	2E-06	89.1 (75.3-105)	177 (153-206)	1.99	2E-05	2.17	0.77	0.36
Il7r/Cd127		36.8 (29.2-46.3)	39.6 (28.4-55.1)	1.08	7E-01	59.2 (50.5-69.3)	22.3 (15.5-32.0)	0.38	2E-04	1.61	0.56	0.35
Tgfb		0.13 (0.09-0.19)	8.02 (3.82-16.8)	60.6	4E-08	1.08 (0.78-1.50)	22.1 (11.5-42.5)	20.4	5E-07	8.18	2.76	0.34
Acod1		1.20 (0.60-2.37)	388 (289-521)	324	2E-10	2.64 (1.72-4.05)	276 (202-378)	105	2E-11	2.21	0.71	0.32
Csf2		0.16 (0.11-0.23)	3.94 (2.09-7.43)	24.9	3E-07	0.05 (0.03-0.07)	0.33 (0.11-0.98)	7.10	4E-03	0.29	0.08	0.28
Stat4		55.4 (50.4-60.8)	110 (95.3-128)	1.99	8E-07	26.4 (21.8-32.0)	14.4 (10.4-19.9)	0.55	6E-03	0.48	0.13	0.27
Dhx58/Lgp2		11.3 (9.76-13.2)	156 (77.1-317)	13.8	2E-06	20.2 (14.3-28.4)	73.1 (55.9-95.5)	3.63	3E-05	1.78	0.47	0.26
Isg15		81.5 (65.6-101)	600 (219-1646)	7.37	2E-03	183 (104-322)	342 (175-668)	1.87	2E-01	2.24	0.57	0.25
Oas1		10.6 (8.90-12.6)	106 (49.4-225)	9.98	3E-05	81.1 (51.9-127)	191 (127-285)	2.35	1E-02	7.67	1.81	0.24
Cgas		1.55 (1.19-2.02)	17.3 (14.3-21.0)	11.2	4E-10	5.53 (4.52-6.77)	13.7 (10.8-17.4)	2.47	3E-05	3.57	0.79	0.22
Gbp4		86.1 (73.9-100)	795 (523-1208)	9.23	4E-08	81.5 (70.5-94.1)	153 (112-209)	1.88	2E-03	0.95	0.19	0.20
Il12		2.85 (2.19-3.71)	11.7 (7.75-17.8)	4.12	4E-05	0.30 (0.17-0.53)	0.25 (0.14-0.43)	0.82	6E-01	0.11	0.02	0.20
ERV Env		913 (661-1261)	3398 (2240-5155)	3.7	2E-04	48.1 (42.9-53.9)	33.1 (25.7-47.5)	0.69	2E-02	0.05	0.01	0.18
Irf7		43.5 (34.1-55.5)	528 (276-1010)	12.1	2E-06	145 (83.0-253)	296 (186-469)	2.04	7E-02	3.33	0.56	0.17
Fos		16.6 (11.9-23.2)	17.3 (9.38-31.8)	1.04	9E-01	20.2 (14.5-28.0)	2.39 (1.61-3.55)	0.12	5E-07	1.21	0.14	0.11
Ifih1/Mda5		8.39 (6.56-10.7)	181 (82.4-395)	21.5	2E-06	43.3 (35.5-52.8)	92.1 (75.8-112)	2.13	6E-05	5.16	0.51	0.10
Cxcl10		0.35 (0.21-0.59)	231 (81.4-655)	659	1E-08	0.26 (0.12-0.59)	16.2 (5.83-44.9)	61.7	1E-05	0.75	0.07	0.094
Mpo		0.33 (0.19-0.57)	19.5 (8.56-44.6)	59.9	6E-07	1.73 (0.71-4.26)	7.91 (2.61-24.0)	4.56	5E-02	5.32	0.41	0.076
Myc		22.4 (18.0-27.7)	294 (209-413)	13.1	3E-09	41.6 (35.9-48.3)	41.4 (25.2-68.1)	1.00	1E+00	1.86	0.14	0.076
Ngp		7.82 (4.03-15.2)	1071 (580-1977)	137	1E-08	130 (77.8-216)	1275 (1022-1589)	9.83	5E-07	16.6	1.19	0.072
Ifit1		10.7 (8.18-13.9)	309 (96.6-991)	29.0	5E-05	53.1 (32.8-85.8)	96.7 (59.0-158)	1.82	1E-01	4.98	0.31	0.063
Mx2		6.29 (5.53-7.16)	270 (158-460)	42.9	1E-09	198 (121-323)	476 (300-757)	2.41	2E-02	31.5	1.76	0.056
Cd69		14.1 (11.5-17.3)	203 (155-266)	14.4	1E-10	39.3 (34.6-44.6)	31.1 (17.3-55.9)	0.79	5E-01	2.78	0.15	0.055
Ccl4		1.84 (1.10-3.09)	217 (126-376)	118	3E-09	117 (75.4-181)	740 (487-1126)	6.33	2E-05	63.5	3.40	0.054
Gzmb		14.7 (9.75-22.1)	1063 (603-1873)	72.4	3E-09	28.8 (15.8-52.6)	103 (56.2-188)	3.57	1E-02	1.96	0.10	0.049
Tnfrsf9/Cd137		0.64 (0.46-0.89)	97.5 (47.3-201)	152	3E-09	0.76 (0.42-1.40)	3.10 (1.62-5.95)	4.06	7E-03	1.19	0.03	0.027
Cd14		44.5 (25.5-77.7)	667 (408-1091)	15.0	2E-06	88.5 (75.5-104)	19.9 (10.4-38.3)	0.23	5E-04	1.99	0.03	0.015
Nos2		0.13 (0.10-0.17)	58.9 (22.1-157)	459	4E-09	0.04 (0.03-0.05)	0.25 (0.09-0.69)	6.16	3E-03	0.31	0.00	0.013
Ifng		0.58 (0.33-1.02)	438 (178-1080)	751	3E-09	0.15 (0.08-0.29)	0.51 (0.14-1.89)	3.30	1E-01	0.26	0.00	0.004

* Gene: Mus musculus reference genome GenBank name/other name in literature. The list includes the 113 coding sequences listed in Methods and two endogenous retrovius (ERV) proteins, Env and Gag-pol.

† Heatmap (red-white-blue scale) of log-transformed "Peromyscus v Mus LPS/control" values (last column). This is ratio of "Peromyscus v Mus LPS FC" (2nd column from right) to "Peromyscus v Mus control FC" (3rd column from right)

‡ Mean unique reads for given gene normalized for reads for Ptprc (Cd45) gene for a sample. The 95% confidence intervals (CI) are asymmetric. Actual [gene]/Ptprc ratios are X 10^-3.

** Other abbreviations: Peromyscus, Peromyscus leucopus; Mus, Mus musculus FC, fold-change; FDR, false discovery rate

"Alternatively-activated" macrophages and "nonclassical" monocytes in *P. leucopus*

While we could not type single cells using protein markers, we could assess relative transcription of established indicators of different white cell subpopulations in whole blood. The present study, which incorporated outbred *M. musculus* instead of an inbred strain, confirmed the previous finding of differences in Nos2, the gene for inducible nitric oxide synthase and Arg1, the gene for arginase 1, expression between *M. musculus* and *P. leucopus* (Figure 5; Table 2). Results similar to the RNA-seq findings were obtained with specific RT-qPCR assays for Nos2 and Arg1 transcripts for *P. musculus* and *M. musculus* (Table 3).

Table 3. RT-qPCR of blood of LPS-treated *P. leucopus* and *M. musculus*

Blood mRNA source	Control mean copies (95% CI)	LPS mean copies (95% CI)	Fold difference LPS/control	*t* test *p* value/Mann-Whitney *p* value
P. leucopus				
Gapdh	1.22 (0.40-3.74) x 10^5	2.38 (1.10-5.16) x 10^5	1.95	0.35/0.49
Nos2	191 (141-260)	138 (61-315)	0.72	0.47/0.53
Arg1	4.62 (3.09-6.92) x 10^3	12.3 (3.22-47.1) x 10^3	2.66	0.18/0.55
M. musculus				
Gapdh	6.10 (2.32-16.0) X 10^6	1.77 (0.80-3.89) X 10^6	0.29	0.06/0.02
Nos2	101 (68-151)	1891 (866-4130)	18.6	<0.00001/0.002
Arg1	27 (15-20)	16 (8-34)	0.59	0.29/0.45

Low transcription of Nos2 in both in controls and LPS-treated *P. leucopus* and an increase in Arg1 with LPS was also observed in another experiment for present study where the dose of LPS was 1 µg/g body mass instead of 10 µg/g and the interval between injection and assessment was 12 h instead of 4 h (Table 4).

Table 4. Targeted RNA-seq of *P. leucopus* blood in 12 h and 1 µg/g LPS experiment

Gene	Control (n=3) mean (95% CI)	LPS (n=3) mean (95% CI)	Fold change	FDR *p* value
Akt1	220 (12-4202)	514 (321-825)	2.3	0.05
Akt2	145 (97-217)	336 (236-478)	2.3	0.04
Arg1	146 (58-367)	2812 (273-28925)	19	0.018
Cd14	82 (12-569)	914 (161-5197)	11	0.05
Cd69	165 (87-310)	68 (14-329)	0.42	0.15
ERV Env	25 (3-242)	40 (7-224)	1.6	0.86
ERV Gag-pol	3085 (132-14695)	2768 (533-1278)	0.9	0.66
Fcgr3/Cd16	40 (25-66)	841 (533-1278)	21	0.008
Gapdh	7176 (3504-15142)	23811 (5827-97306)	3.3	0.07
Gbp4	97 (6-1551)	439 (33-5819)	4.5	0.05
Ifit1	367 (51-2663)	1373 (374-5047)	3.7	0.05
Ifng	0 (0-0)	0 (0-0)	.	.
Il1b	258 (18-3652)	1432 (183-11220)	5.6	0.1
Irf7	121 (93-157)	11405 (530-245616)	94	0.003
Isg15	429 (184-1001)	19505 (11140-34152)	45	0.005
Mx2	157 (73-341)	1310 (323-5315)	8.3	0.04
Nos2	0 (0-0)	0 (0-0)	.	.
Oas1	65 (31-138)	1458 (367-5795)	22	0.03
Rigi/Ddx58	38 (3-504)	173 (35-845)	4.5	0.07
Saa3	2 (0-250)	6683 (1494-29896)	3372	0.03
Slpi	6 (1-46)	779 (326-1864)	123	0.03
Sod2	180 (54-607)	3406 (698-16633)	19	0.03

In addition to the differences in Nos2 and Arg1 expression for typing macrophage and monocyte subpopulations, there are also the relative expressions of three other pairs of genes: (1) IL12 and IL10, where a lower IL12/IL10 ratio is more characteristic of alternatively activated or M2 type [68, 90]; (2) the proto-oncogene kinases Akt1 and Akt2, where the associations are Akt1 with M2-type and Akt2 with M1-type macrophages [1, 91]; and (3) CD14 and CD16 (low affinity immunoglobulin gamma Fc region receptor III; Fcgr3), where low expression of CD14 and high expression of CD16/Fcgr3 is associated with "non-classical" monocytes [70]. There is evidence that nonclassical monocytes can change to M2-type macrophages [42].

These four relationships, which are presented as log-transformed ratios of Nos2/Arg1, IL12/IL10, Akt1/Akt2, and CD14/CD16, are shown in Figure 6. We confirmed the difference between *P. leucopus* and *M. musculus* in the ratios of Nos2/Arg1 and IL12/IL10 [3] with outbred mice and normalization for white cells. In both species the Akt1/Akt2 ratio declined in LPS-treated animals,

but for *P. leucopus* the ratio remained > 1.0 even among LPS-treated animals, while in the blood of *M. musculus* the ratio was < 1.0 at baseline and declined further in the LPS-treated animals.

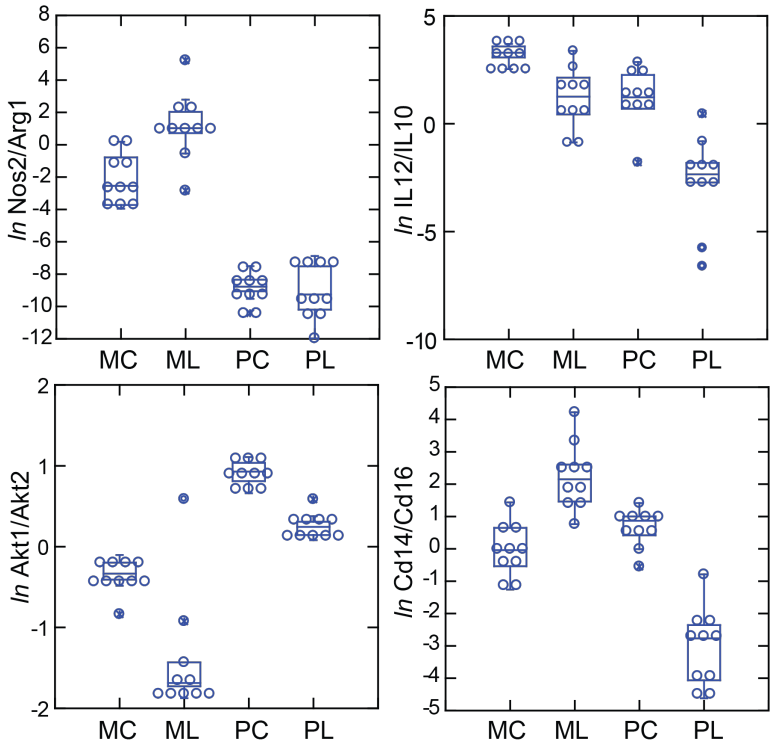

Figure 6. Box plots of log-transformed ratios of four pairs of gene transcripts from targeted RNA-seq analysis of blood of *P. leucopus* (P) or *M. musculus* (M) with (L) or without (C) treatment with LPS. The values are from Table S4. Upper left, Nos2/Arg1. Upper right, IL12/IL10. Lower left, Akt1/Akt2. Lower right, Cd14/Cd16.

An ortholog of Ly6C [13], a protein used for typing mouse monocytes and other white cells, has not been identified in *Peromyscus* or other Cricetidae family members. Therefore, for this study the comparison with Cd14 is with Cd16 or Fcgr3, which deermice and other cricetines do have. In mice the Cd14/Cd16 ratio increased from baseline in the LPS group. In the deermice the ratio in control animals was midway between the two groups of mice but there was a marked decrease in the LPS-treated deermice (Figure 6). This was not associated with a fall in the absolute numbers or percentages of monocytes in the blood of these animals.

Taken together, the Nos2-Arg1, Il12-Il10, Akt1-Akt2, and CD14-CD16 relationships document a disposition toward alternatively-activated macrophages and nonclassical monocytes in *P. leucopus* both before and after exposure to LPS. This contrasts with profiles consistent with a predominance of classically-activated macrophages and classical monocytes in mice.

Interferon-gamma and interleukin-1 beta dichotomy between deermice and murids

For mice the Ifng transcript was one of the top ranked DEGs by both fold-change and adjusted *p* value by genome-wide RNA-seq (Table 2). In contrast, for *P. leucopus* Ifng was far down the list, and the comparably ranked DEG instead was Il1b. This inversion of relationships between two pro-inflammatory cytokines was confirmed by analysis of the individual animals of both species (Figure 7). There was little or no detectable transcription of Ifng in the blood of deermice in which Il1b expression was high. There was also scant to no transcription of Ifng in the blood of *P. leucopus* 12 h after injection of LPS (Table 4).

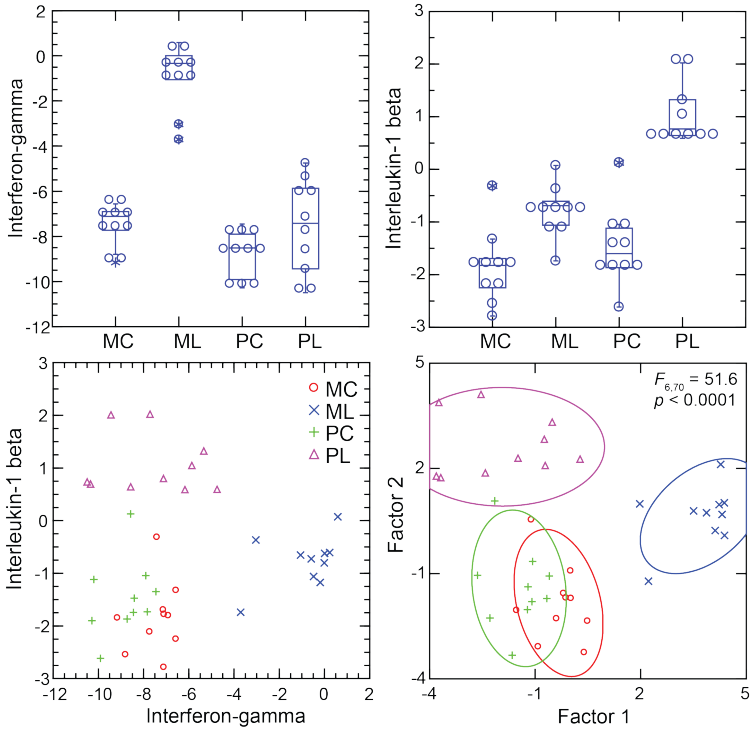

Figure 7. Transcripts of interferon-gamma and interleukin-1 beta by targeted RNA-seq of the blood of *P. leucopus* (P) or *M. musculus* (M) with (L) or without (C) treatment with LPS. The top panels are box plots of the individual values. The lower left panel is a scatter plot of interleukin-1 β on interferon- γ values. The lower right panel is a Discriminant Analysis of these pairs of values where Factor 1 corresponds to interferon-gamma, and Factor 2 corresponds to interleukin-1 beta. Values for analysis are in Table S4.

The up-regulation of Ifng within 4 hours of exposure to LPS was not limited to the species *M. musculus*. In an experiment with the rat *R. norvegicus*, we used two different LPS doses (5 µg/g and 20 µg/g), but the same 4 h endpoint and whole blood as the sample. Both groups of LPS-treated rats had lowered total white blood cells and, like the mice, lower neutrophil-to-lymphocyte ratios compared to controls (Table 5). There were also elevations of interferon-gamma, interleukin-6 and interleukin-10 proteins from undetectable levels in the blood of the treated rats (Dryad Table D5). The values for rats receiving 5 µg/g or 20 µg/g doses were similar (Figure S3), so these groups were combined. By targeted RNA-seq there were 24x fold-changes between the LPS-treated rats and control rats for Ifng and Nos2 but only ~3x fold-change for Il1b (Table 5).

Table 5. Hematology, cytokines, and targeted RNA-seq of LPS-treated and control rats

Variable	Control (n=5) mean (95% CI)*	LPS (n=11) mean (95% CI)*,†	Fold change	FDR *p* value
Hematology				
Hematocrit (%)	48 (46-50)	48 (46-49)	1.0	1E+00
White blood cells	7660 (7200-8310)	4980 (2020-7940)	0.75	2E-01
Neutrophils	3680 (3260-4090)	1410 (520-2290)	0.38	4E-03
Lymphocytes	3170 (3010-3330)	2830 (1230-4430)	0.89	8E-01
Neutrophil/lymphocyte	1.17 (1.01-1.33)	0.49 (0.44-0.55)	0.42	7E-09
Plasma cytokines (pg/ml)				
Interleukin-6	0 (0-0)	36933 (21676-52190)	.	5E-15
Interleukin-10	9 (1-17)	640 (477-802)	71	2E-09
Interferon-gamma	0 (0-0)	9091 (7126-11056)	.	9E-20
Targeted RNA-seq				
Akt1	35.8 (29.8-42.9)	24.3 (21.5-27.5)	0.68	4E-03
Akt2	50.8 (44.9-57.4)	109 (95.2-125)	2.2	9E-06
Arg1	0.04 (0.02-0.08)	0.21 (0.10-0.44)	4.8	2E-02
Cd14	7.7 (5.3-11.2)	43.4 (29.6-63.6)	5.6	9E-05
Cd177	0.89 (0.43-1.8)	190 (143-251)	213	2E-10
Cd3	32.3 (27.7-37.6)	21.9 (18.5-25.8)	0.68	1E-02
Cd69	17.9 (16.7-19.2)	58.9 (49.1-70.7)	3.3	9E-07
Cgas	1.5 (1.3-1.6)	12.8 (10.8-15.1)	8.7	3E-10
Cxcl10	0.43 (0.34-0.56)	130 (93.7-181)	302	1E-11
Dhx58	7.1 (6.7-7.6)	113 (97.3-130)	15.8	3E-12
ERV Env	8.4 (7.5-9.3)	713 (624-815)	85.3	1E-14
ERV gag-pol	6.0 (5.4-6.7)	506 (449-570)	84.3	7E-15
Fcgr2a	114 (87.0-150)	764 (631-925)	6.7	4E-08
Fcgr2b	32.5 (24.6-43.1)	161 (127-204)	4.9	2E-06
Fcgr3/Cd16	15.2 (13.6-17.0)	13.9 (11.8-16.3)	0.91	5E-01
Gapdh	327 (237-451)	1643 (1385-1949)	5.0	2E-07
Gbp4	35.7 (33.6-38.0)	269 (237-306)	7.5	3E-11
Ibsp	0.41 (0.31-0.55)	0.61 (0.47-0.80)	1.5	1E-01
Ifih1	18.7 (17.1-20.4)	165 (149-184)	8.8	2E-12
Ifit1	102 (70.0-147)	756 (677-844)	7.4	3E-09
Ifng	0.47 (0.32-0.67)	10.3 (6.4-16.5)	22.1	1E-06
Il10	0.12 (0.07-0.21)	4.5 (3.4-5.8)	38.2	5E-09
Il12	0.07 (0.04-0.11)	3.2 (2.0-4.9)	45.9	7E-08
Il1b	58.6 (39.7-86.4)	618 (503-760)	10.6	2E-08
Il6	0.06 (0.05-0.08)	4.4 (2.9-6.6)	70.9	6E-09
Irf7	44.8 (36.9-54.3)	443 (372-528)	9.9	6E-10
Isg15	15.6 (13.1-18.7)	624 (534-729)	39.9	6E-13
Itgam?Cd11b	66.3 (52.5-83.7)	208 (161-269)	3.1	9E-05
Mmp8	75.2 (50.4-112)	519 (438-615)	6.9	7E-08
Mx2	40.7 (35.9-46.2)	900 (780-1039)	22.1	1E-12
Nos2	32.4 (17-60.6)	2990 (2491-3589)	92.4	1E-10
Oas1	23.1 (18.8-28.4)	151 (140-164)	6.6	3E-11
Rigi/Ddx58	8.6 (7.8-9.4)	151 (135-168)	17.6	1E-13
S100a9	298 (190-466)	2884 (2269-3666)	9.7	2E-07
Saa1	0.60 (0.49-0.73)	699 (552-884)	1167	4E-14
Slpi	20.2 (13.1-31.3)	262 (197-347)	12.9	1E-07
Sod2	63.8 (51.1-79.6)	901 (759-1070)	14.1	2E-10
Tlr4	5.3 (4.6-6.0)	20.1 (17.2-23.6)	3.8	8E-08
Tnf	1.1 (0.63-1.9)	78.8 (62.6-99.1)	72.8	2E-10
Ratios				
Akt1/Akt2	0.70 (0.65-0.76)	0.22 (0.19-0.25)	0.31	2E-08
Cd14/Fcgr3	0.51 (0.34-0.76)	3.14 (2.26-4.36)	6.16	1E-05
IL12/IL10	0.54 (0.22-1.37)	0.70 (0.51-0.95)	1.30	5E-01
Nos2/Arg1	741 (403-1362)	14244 (7615-26646)	19.2	5E-05

* For targeted RNA-seq it is mean unique reads for given gene normalized for reads for Ptprc (Cd45) gene for a sample. The 95% confidence intervals (CI) are asymmetric. Actual [gene]/Ptprc ratios are X
† The results for rats receiving 5 μg/g (n=6) and 20 μg/g (n=5) were combined

We asked why the Infg response observed in CD-1 mice and rats here was not as pronounced in BALB/c mice [3]. Accordingly, we used the RNA-seq reads from the prior study in combination with the reads of the present study and carried out targeted RNA-seq (Figure S4). The BALB/c inbred mice had, like the CD-1 mice, modest elevations of Il1b transcription. Ifng expression was also elevated in the BALB/c animals but not to the degree noted in CD-1 mice or rats. One explanation is an inherent difference of BALB/c mice from other strains in their lower interferon-gamma response to LPS [47, 84].

Interferon-gamma and inducible nitric oxide synthase

Interferon-gamma is a determinant of Nos2 expression [55, 81]. So, the scant transcription of Ifng in *P. leucopus* conceivably accounted for the low expression of Nos2 in that species. The analysis shown in upper left panel of Figure 8 shows a tight correlation between the levels of transcription of Ifng and Nos2 for both species and both experimental conditions (Figure S5). A significant

correlation was also observed for the combined set of animals between the ratios of Nos2 to Arg1 and Ifng to Il1b (upper right panel), an indication of co-variation between Ifng expression and macrophage polarization.

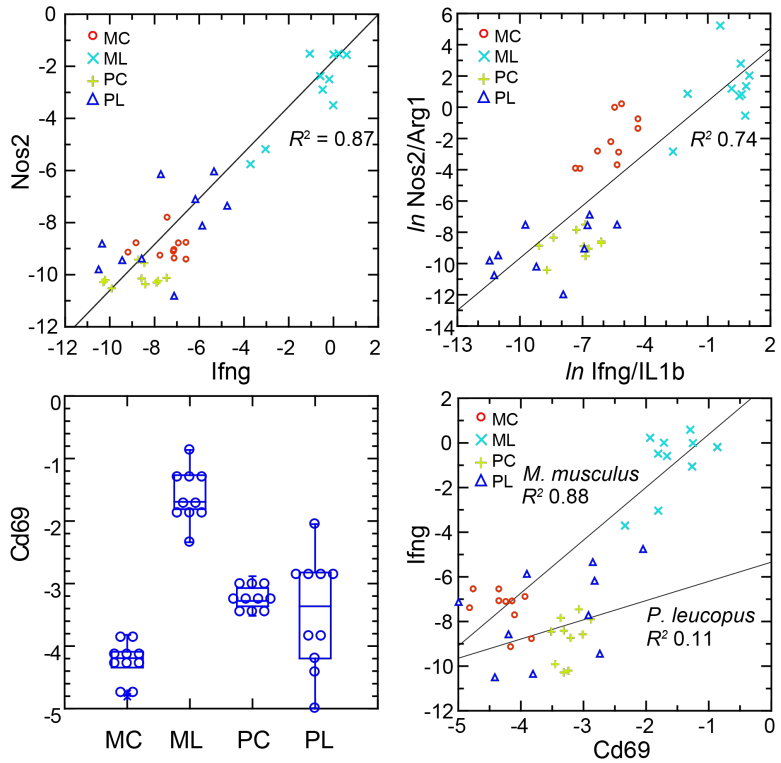

Figure 8. Normalized transcripts of Nos2, Ifng, and Cd69 in targeted RNA-seq analysis of blood of *P. leucopus* (P) or *M. musculus* (M) with (L) or without (C) treatment with LPS. Upper left: scatter plot of individual values for Nos2 on Ifng with linear regression curve and coefficient of determination (R^2). Upper right: natural logarithm (*ln*) of ratios of Nos2/Argi1 on Ifng/IL1b with regression curve and R^2. Lower left: Box plots of individual values of normalized transcripts of Cd69. Lower right: Scatter plot of Ifng on Cd69 with separate regression curves and R^2 values for *M. musculus* and *P. leucopus*. Values for analysis are in Table S4. Box plots for Nos2 and Arg1 are provided in Figure S5, and box plots for Ifng and Il1b are provided in Figure 7.

The plausible sources of Ifng mRNA in whole blood are T-cells, Natural Killer cells, and Type 1 Innate Lymphoid Cells [75]. A DEG for *M. musculus* by both genome-wide and targeted RNA-seq (Table 2; Table S1) was Cd69, a C-type lectin protein and an early activation antigen for these cells [38]. In *P. leucopus* transcription Cd69 occurred in the blood of control *P. leucopus*, but it was the same or only marginally different for the LPS-treated animals (lower left panel). In contrast, in *M. musculus* the baseline transcription of Cd69 was below that of *P. leucopus*, but in the LPS-treated mice it was many fold higher. In mice transcripts for Cd69 correlated tightly with Ifng transcription, while in the deermice there was little correlation between Cd69 and Ifng expression at those low levels (lower right panel).

The findings are consistent with CD69-positive cells being a source of Ifng in mice. Cd69 transcription was comparatively higher in control deermice than in control mice, so we presume that deermice have CD69-positive cells at baseline. One explanation then for the comparatively few Ifng transcripts in the deermice after LPS is a diminished responsiveness of these cells. Tlr4 expression increased ~3 -fold more in *P. leucopus* than in *M. musculus* after LPS (Table 2), but the magnitude of the decline in expression of Cd14 in deermice than mice was even greater. CD14 is required for LPS-stimulated signaling through surface TLR4 [58], and, as such, its decreased availability for this signaling pathway is a possible explanation for the moderated response to LPS in *P. leucopus*.

Interferon-stimulated genes and RIG-I-like receptors

As noted, GO terms differentiating mice from deermice included "response to interferon-beta" and "response to virus" (Figure 3). There was also the example of Mx2, an ISG with anti-viral activity on its own, that showed a greater fold-change from baseline in mice than in deermice (Figure 5). Five other ISGs--guanylate binding protein 4 (Gbp4), interferon-induced protein with tetratricopeptide repeat (Ifit1), interferon regulatory factor 7 (Irf7), ubiquitin-type modifier ISG15 (Isg15), and 2'-5' oligoadenylate synthase 1A (Oas1a)—had higher transcription in all the LPS-treated animals. But the magnitude of fold change was less in the deermice, ranging from 6-25% of what it was in the LPS group of mice (Table 2; Figure S6).

The up-regulation of these ISGs was evidence of an interferon effect, but transcripts for interferon-1 beta (Ifnb) or -alpha (Ifna) themselves were scarcely detectable in deermice or mice in the blood under either condition. We then considered pattern recognition receptors (PRR) that might be part of a signaling pathway leading to ISG expression. Among the DEGs from the genome-wide analyses were four cytoplasmic PRRs: (1) Rigi (formerly Ddx58), which encodes the RNA helicase retinoic acid-inducible I (RIG-I); (2) Ifih1, which encodes interferon induced with helicase C domain 1, also known as MDA5 and a RIG-I-like receptor; (3) Dhx58, also known LGP2 and another RIG-I-like receptor; and (4) cGAS (cyclic GMP-AMP synthase), which is part of the cGAS-STING sensing pathway (Table S4).

	Cgas	Dhx58	Ifih1	Rigi	Gbp4	Irf7	Isg15	Mx2	Oas1
Cgas	1.00	0.70	0.78	0.40	0.46	0.63	0.39	0.77	0.61
Dhx58		1.00	0.86	0.80	0.76	0.79	0.61	0.58	0.62
Ifih1			1.00	0.54	0.59	0.79	0.61	0.77	0.75
Rigi				1.00	0.83	0.52	0.43	0.20	0.26
Gbp4					1.00	0.52	0.43	0.24	0.24
Irf7						1.00	0.81	0.71	0.77
Isg15							1.00	0.48	0.59
Mx2								1.00	0.87
Oas1									1.00

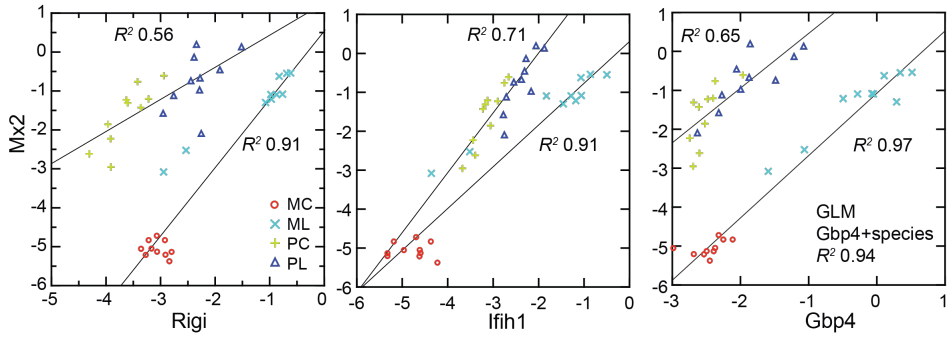

Figure 9. Co-variation between transcripts for selected PRRs and ISGs in the blood of *P. leucopus* (P) or *M. musculus* (M) with (L) or without (C) LPS treatment. Top panel: matrix of coefficients of determination (R^2) for combined *P. leucopus* and *M. musculus* data. PRRs are indicated by yellow fill and ISGs by blue fill on horizontal and vertical axes. Shades of green of the matrix cells correspond to R^2 values, where cells with values less than 0.30 have white fill and those of 0.90-1.00 have deepest green fill. Bottom panels: scatter plots of log-transformed normalized Mx2 transcripts on Rigi (left), Ifih1 (center), and Gbp4 (right). The linear regression curves are for each species. For the right-lower graph the result from the General Linear Model (GLM) estimate is also given. Values for analysis are in Table S4; box plots for Gbp4, Irf7, Isg15, Mx2, and Oas1 are provided in Figure S6.

All four cytoplasmic PRRs were upregulated in the blood of LPS-treated mice and deermice (Table 2). But, again, for each of them the magnitude of fold change was less by 50-90% in treated *P. leucopus* than in *M. musculus*. The coefficients of determination for the 6 ISGs and the 4 PRRs are provided in Figure 9. For most of the pairs there was evidence of covariation across all 40 animals. When the correlation was low across all the data, e.g. between the ISG Mx2 and the PRR Rigi or the ISGs Mx2 and Gbp4, it was high within a species.

These findings were evidence that pathways in *P. leucopus* for PRR signaling and ISG expression functioned similarly to those in *M. musculus* but differed under these experimental conditions in magnitude of the changes, being more moderate in the deermice.

Endogenous retroviruses in deermice, mice, and rats after LPS exposure

The six ISGs are nonexclusive consequences of activity of type 1 interferons. What we could document was the association of transcription of the gene for the cytoplasmic PPRs, including RIG-I, and the ISGs in both species, as well as the distinction between deermice in the magnitude of the responses of both PRRs and ISGs. These findings led us to ask could be a pathogen-associated molecular pattern (PAMP) for signaling pathways leading to expression of type 1 interferons.

One of these is endogenous retroviruses (ERV). The activity of these diverse, abundant, and pervasive elements have been recognized as one of the drivers of innate immune responses to a microbe [41, 51, 76]. Our attention was drawn to ERVs by finding in the genome-wide RNA-seq of LPS-treated and control rats. Two of the three highest scoring DEGs by FDR *p* value and fold-change were a *gag-pol* polyprotein of a leukemia virus with 131x fold-change from controls and a mouse leukmia virus (MLV) envelope (Env) protein with 62x fold-change (Dryad Table D5).

We returned to the mouse and deermouse data. There were four MLV or other ERV Env proteins among the 1266 genome-wide RNA-seq DEGs for *M. musculus*. But, there was no ERV Env protein identified as such among the 1154 DEGs identified for *P. leucopus* (Table S1). One possible explanation for the difference was an incomplete annotation of the *P. leucopus* genome. We took three approaches to rectify this. The first was to examine the DEGs for *P. leucopus* that encoded a polypeptide ≥ 200 amino acids and was annotated for the genome as "uncharacterized". A search with these candidates of both the virus and rodent proteins databases identified two that were homologous with *gag-pol* polyproteins of ERVs, mainly leukemia viruses, of mammals.

For a second approach we carried out a de novo transcript assembly of mRNA reads from blood of LPS-treated and control *P. leucopus* and used the resultant contigs as the reference set for RNA-seq analysis. This identified two contigs that were measurably transcribed in the blood, differentially expressed between conditions, and were homologous to ERV sequences. One was revealed to be an Env protein that was identical to a *P. leucopus* protein annotated as "MLV-related proviral Env protein" (XP_037065362). The second was a *gag-pol* protein. The latter was near-identical to the *gag-pol* protein identified by the first approach.

The third approach was to scan the *P. leucopus* genome for nonredundant sequences, defined as <95% identity, that were homologous with ERV *gag-pol* sequences, which are not typically annotated because of masking for repetitive sequences. This analysis yielded 615 unique sequences. These were used in turn as a reference set for RNA-seq. There were 4 sequences that met the criterion of FDR *p* value <0.01. Three were transcribed at 5- to 40-fold higher levels in LPS-treated deermice than in controls. But all three, as well as the fourth, a down-regulated DEG, were ERV relics with truncations, frame shifts, and in-frame stop codons. These were assessed as non-coding RNAs and not further pursued in this study.

To represent *P. leucopus* in a targeted RNA-seq comparison with mice and rats we settled on the Env protein and *gag-pol* coding sequences identified present in the blood mRNA and as DEGs. Representing *M. musculus* were highest ranked MLV Env and *gag-pol* protein sequences among the DEGs. For rats we chose Env and *gag-pol* proteins that were second and third ranked DEGs identified in the genome-wide RNA-seq. Because of length differences for the coding sequences, the unit used for cross-species analysis was reads per kilobase before normalization for Ptprc transcription.

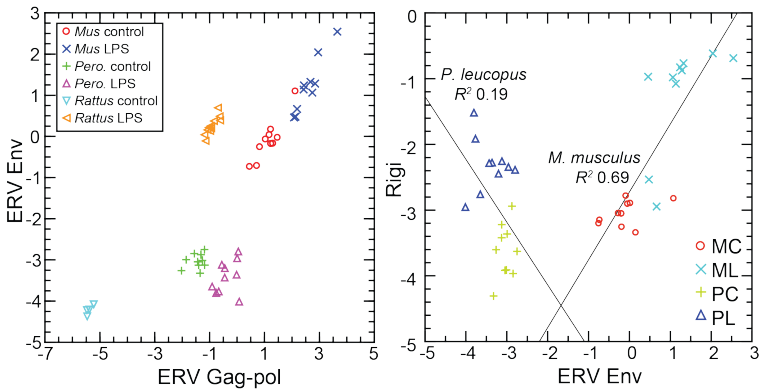

Figure 10. Scatter plots of endogenous retrovirus (ERV) Env and Gag-pol protein gene transcription (left) and association of ERV Env with Rigi transcription (right) in the blood of *P. leucopus* (*Pero*; P), *M. musculus* (*Mus*; M), or *R. norvegicus* (*Rattus*) with (L) or without (control; C) treatment with LPS. In right panel the linear regression curve and coefficients of determination (R^2) for *P. leucopus* and *M. musculus* are shown. Values for analysis are in Table S4; box plots for ERV Env and ERV Gag-pol are provided in Figure S7.

The left panel of Figure 10 shows the striking transcriptional fold-change in LPS-treated rats of both Env and *gag-pol* sequences over controls. Of lesser magnitude but no less significant was the fold-change observed *M. musculus* for both Env and *gag-pol* sequences. In both mice and rats Env and *gag-pol* read values were highly correlated across conditions. In contrast, in *P. leucopus* the magnitudes of fold-change upwards for *gag-pol* was less than in mice or rats, and transcription of the Env protein sequence was actually lower in LPS-treated animals than in controls. While there was a tight association between Env protein and the PRR Rigi transcription in the *M. musculus*, this was not observed in *P. leucopus*. Rigi transcription was moderately higher at the time that Env protein's transcription was lower in the LPS group.

Borrelia hermsii infection of *P. leucopus*

The phenomena reported so far were consequences of exposures to a particular PAMP--bacterial lipopolysaccharide with its hallmark lipid A moiety--recognized by a particular PRR, TLR4. While the focus was primarily on events downstream from that initial signaling, we asked in a concluding study whether the profile observed in *P. leucopus* applied in circumstances when the PAMP or PAMPs did not include LPS. This question is germane, given *P. leucopus'* role as a natural host for *B. burgdorferi*. This organism and other members of the spirochete family *Borreliaceae* do not have LPS [5, 88], but they have abundant lipoproteins, which are agonists for TLR2 in a heterodimer with TLR1 [80]. *B. burgdorferi* is transiently blood-borne at low densities in *P. leucopus*, but in its life cycle *B. burgdorferi* is mainly tissue-associated in vertebrate hosts [6]. We previously observed that the blood of *B. burgdorferi*-infected *P. leucopus* manifested few DEGs in comparison to skin [52]. More comparable to the LPS experimental model is infection of *P. leucopus* with a relapsing fever *Borrelia* species, which commonly achieve high densities in the blood. *P. leucopus* is a reservoir for *Borrelia miyamotoi*, which causes hard tick-borne relapsing fever [6], and the related *P. maniculatus* is a natural host for the soft tick-borne relapsing fever agent *B. hermsii* [43].

Accordingly, we used blood RNA-seq reads, which were taken from a prior study of *B. hermsii* infection of *P. leucopus* [3], for targeted analysis with the same reference set employed for the LPS analyses (Table 6 and Table S5). The blood samples were taken from infected and uninfected animals on day 5, when bacteremia was at its peak, as documented by microscopy of the blood, qPCR of the spleen, and transcripts of a *B. hermsii* plasmid in the RNA extracts of the blood. As expected for *B. hermsii* infection [24], the spleen was enlarged in infected animals.

Table 6. Targeted RNA-seq of *P. leucopus* with and without *Borrelia hermsii* infection

Variable	Uninfected (n=3) mean (95% CI)*	Infected (n=4) mean (95% CI)*	Fold change	FDR *p* value
B. hermsii qPCR spleen	.	13615 (1882-98476)	.	.
B. hermsii reads blood	.	3487 (743-16362)	.	.
% spleen/body mass	0.15 (0.12-0.19)	0.36 (0.26-0.51)	2.4	1E-02
Targeted RNA-seq				
Akt1	184 (135-253)	347 (191-630)	1.88	3E-01
Akt2	92.9 (72.4-119)	141 (89.4-222)	1.52	3E-01
Arg1	247 (96.9-630)	1375 (848-2230)	5.57	4E-02
Cd14	308 (119-799)	598 (357-1002)	1.94	3E-01
Cd177	2.11 (0.71-6.27)	35.9 (11.9-108)	17.0	4E-02
Cd3	86.9 (77.7-97.2)	56.2 (16.4-192)	0.65	6E-01
Cd69	133 (114-155)	65 (33.6-128)	0.49	2E-02
Cgas	8.87 (5.40-14.6)	16.8 (8.99-31.4)	1.89	3E-01
Cxcl10	0.33 (0.14-0.76)	4.85 (2.74-8.59)	14.7	2E-02
Dhx58	22.0 (9.26-52.4)	37.0 (13.3-103)	1.68	6E-01
ERV Env	26.8 (22.4-32.1)	29.2 (14.8-57.8)	1.09	9E-01
ERV gag-pol	1853 (1351-2542)	1578 (820-3037)	0.85	8E-01
Fcgr2a	44.8 (24.0-83.6)	715 (303-1689)	16.0	2E-02
Fcgr2b	47.3 (30.2-74.3)	578 (167-2000)	12.2	5E-02
Fcgr3 (Cd16)	30.6 (18.6-50.4)	392 (171-897)	12.8	2E-02
Gapdh	1985 (1142-3447)	5366 (2383-12081)	2.70	2E-01
Gbp4	126 (82.3-193)	289 (130-644)	2.30	3E-01
Ibsp	0.81 (0.56-1.16)	358 (95-1350)	444	1E-02
Ifih1	48.5 (31.9-73.7)	49.1 (26.8-89.7)	1.01	1E+00
Ifit1	223 (107-465)	604 (303-1203)	2.71	2E-01
Ifng	0.58 (0.09-3.92)	2.28 (0.86-6.06)	3.94	3E-01
Il10	0.25 (0.07-0.87)	1.49 (0.31-7.28)	5.94	3E-01
Il12	0.43 (0.23-0.81)	1.13 (0.45-2.88)	2.63	3E-01
Il1b	477 (174-1308)	2828 (1325-6034)	5.93	7E-02
Il6	0.51 (0.18-1.39)	1.80 (0.61-5.28)	3.55	3E-01
Irf7	93.3 (13.4-65)	626 (196-1998)	6.71	2E-01
Isg15	302 (30.1-3030)	1922 (623-5934)	6.36	3E-01
Itgam (Cd11b)	72.2 (44.5-117)	322 (211-492)	4.45	2E-02
Mmp8	7.1 (2.74-18.6)	537 (148-1952)	75.2	2E-02
Mx2	152 (48.6-476)	167 (48.0-582)	1.10	9E-01
Nos2	0.16 (0.08-0.30)	0.32 (0.13-0.80)	2.01	4E-01
Oas1	51.3 (6.75-390)	159 (39.2-643)	3.10	5E-01
Rigi (Ddx58)	38.7 (18.9-79.2)	55.7 (33.9-91.5)	1.44	5E-01
S100a9	1739 (657-4596)	18430 (6546-51883)	10.6	5E-02
Saa3	0.49 (0.13-1.87)	212 (25.9-1733)	431	2E-02
Slpi	0.41 (0.18-0.95)	166 (49.0-566)	401	1E-02
Sod2	104 (51.4-211)	2011 (804-5028)	19.3	2E-02
Tlr1	21.4 (15.0-30.4)	111 (53.9-230)	5.21	4E-02
Tlr2	83.2 (59.7-116)	371 (234-587)	4.46	2E-02
Tlr4	44.8 (26.1-77.0)	256 (138-474)	5.71	3E-02
Tnf	2.86 (1.64-4.96)	78.8 (38.8-160)	27.6	1E-02
Ratios				
Akt1/Akt2	2.0 (1.7-2.3)	2.5 (2.1-2.9)	1.25	1E-01
Cd14/Fcgr3	11.3 (4.8-17.9)	1.7 (0.72-2.8)	0.15	2E-02
IL12/IL10	2.3 (0.00-5.0)	2.8 (0.0-7.6)	1.21	9E-01
Nos2/Arg1	0.001 (0.0-0.002)	0.0001 (0.0-0.0004)	0.28	2E-01

* For targeted RNA-seq it is mean unique reads for given gene normalized for reads for Ptprc (Cd45) gene for a sample. The 95% confidence intervals (CI) are asymmetric. Actual [gene]/Ptprc ratios are X 10^-3.

Similarities in the profiles for the LPS-treated and *B. hermsii*-infected deermice were as follows: (1) low levels of transcription of Nos2 and Ifng that contrasted with the high levels for Arg1 and Il1b in the same animals, (2) maintenance of Akt1/Akt2 > 1.0 under both conditions, (3) reduction of the Cd14/Cd16 ratio, (4) decreased transcription of Cd69, and (5) stable, low transcription of ERV Env and gag-pol loci with only marginal increases in transcription of ISGs and RIG-I-like receptors. Other equivalences under the two experimental conditions included increases in expression of genes for superoxide dismutase 2, low-affinity Fc gamma receptors, and secretory leukocyte protease inhibitor. Thus, the responses that distinguish deermice are not confined to the singular case of LPS as the elicitor.

DISCUSSION

Study limitations

The approach was forward and unbiased, looking for differences between species broadly across their transcriptomes. The findings lead to hypotheses, but reverse genetics in service of that testing was not applied here. In selective cases we could point to supporting evidence in the literature

on *M. musculus* and the phenotypes of relevant gene knockouts, but there are no such resources for *Peromyscus* as yet. The resource constraint also applies to the availability of antibodies for use with *Peromyscus* for immunoassays for specific proteins, e.g. interferon-gamma, in serum, or for cell markers, e.g. CD69, for flow cytometry of white blood cells.

While a strength of the study was use of an outbred population of *M. musculus* to approximate the genetic diversity of the *P. leucopus* in the study, this meant that some genes of potential relevance might have gone undetected, i.e. from type II error. The variances for a sample of genetically diverse outbred animals, like the LL stock of *P. leucopus* [52, 53], would be expected to be greater than for the same sized sample of inbred animals. For some traits, especially ones that are complex or under balancing selection, even sample sizes of 10 in each group may not have provided sufficient power for discrimination between deermice and mice. For the same reason differences between sexes of a species in their responses might have been undetected. The interpretations applied to mixed-sex groups of deermice and mice. Expression strongly associated with female or male sex could have yielded an average fold change for the whole group that fell below the screen's threshold.

The parameters for the experiment of LPS dose, the route, and duration of experiment each might have had different values under another design. Those particular choices were based on past studies of deermice and mice [3, 49]. In another experiment we found that with doses twice or half those given the deermice the responses by rats to the different doses were indistinguishable by hematology, cytokine assays, and RNA-seq. Thus, there seems to be some latitude in the dose and still achieving replication. We obtained similar results for *P. leucopus* when we looked at a replicate of the experiment with the same conditions [3], when the dose was lower and duration lengthened to 12 h (this study). The analysis here of the *B. hermsii* infection experiment also indicated that the phenomenon observed in *P. leucopus* was not limited to a TLR4 agonist.

While the rodents in these experiments were housed in the same facility and ate the same diet, we cannot exclude inherent differences in gastrointestinal microbiota between species and individual outbred animals as co-variables for the experimental outcomes. We reported differences between the LL stock *P. leucopus* and BALB/c *M. musculus* of the same age and diet in their microbiomes by metagenomic analysis and microbiologic means [61]. This included a commensal *Tritrichomonas* sp. in *P. leucopus* but not in the *M. musculus* in the study. The presence of these protozoa affects innate and adaptive immune responses in the gastrointestinal tract [19, 29], but it is not clear whether there are systemic consequences of colonization by this flagellate.

LPS, ERVs, and interferons

The results confirm previous reports of heightened transcription of ERV sequences in mice or mouse cells after exposure to LPS [35, 44, 87]. Here we add the example of the rat. The LPS was administered in solution and not by means of membrane vesicles. The sensing PRR presumably was surface-displayed, membrane-anchored TLR4 [58]. It follows that a second, indirect of LPS on the mouse is through its provocation of increased ERV transcription intracellularly. ERV-origin RNA, cDNA and/or protein would then be recognized by a cytoplasmic PRR. RIG-I was one associated with ERV transcription in this study. Kong et al. reported that LPS stimulated expression of Rigi in a mouse macrophages but did not investigate ERVs for an intermediary function in this phenomenon [46]. As was demonstrated for LINE type retrotransposons in human fibroblasts, intracellular PRR signaling can trigger a type 1 interferon response [25]. The combination of these two signaling events, i.e. one through surface TLR4 by LPS itself and another through intracellular PPR(s) by to-be-defined ERV products, manifested in mice and rats as a response profile that had features of both a response to a virus with type 1 interferon and ISGs and a response to a bacterial PAMP like LPS with acute phase reactants such as calprotectin and serum amyloid.

This or a similar phenomenon has been observed under other circumstances. In humans there was heightened transcription of retrotransposons in patients with septic shock [63], as well as in peripheral blood mononuclear cells from human subjects experimentally injected with LPS [74]. Bacteria like *Staphylococcus epidermidis* that express TLR2 agonists, such as lipoteichoic acid,

promoted expression of ERVs, which in turn modulated host immune responses [51]. A synthetic analog of a *B. burgdorferi* lipoprotein activated human monocytic cells and promoted replication of the latent HIV virus in cells that were persistently infected [72].

P. leucopus does not fit well with this model. Instead of the prominent interferon-gamma response observed in mice and rats, there were prominent responses of interleukin-1 beta and genes associated with neutrophil activation. Instead of the much heightened expression of ISGs, like Mx2 and Isg15, in mice treated with LPS, the deermice under the same condition had a more subdued ISG transcription profile. Instead of increased expression of ERV Env protein sequences in blood of mice and rats treated with LPS, there was decreased transcription of the homologous MLV Env gene in like-treated *P. leucopus*.

This suppression in the deermice may be attributable to defensive adaptations of *Peromyscus* to repeated invasions of endogenous retroviruses, as Gozashti et al. has proposed for *P. maniculatus* [32]. This includes expanding the repertoire of silencing mechanisms, such as Kruppel-associated box (KRAB) domain-containing zinc finger proteins [97]. Like *P. maniculatus*, *P. leucopus* has an abundance of Long Terminal Repeat retrotransposons, several named for their endogenous retrovirus heritages [52]. Our initial analysis of the *P. leucopus* genome reported a depletion of KRAB domains compared to Muridae [52]. But a subsequent annotation round identified several genes for KRAB domain zinc finger proteins in *P. leucopus*, including Zfp809 (XP_006982432), which initiates ERV silencing [95], and Zfp997 (XP_037067826), which suppresses ERV expression [89]. Another possible adaptation in *P. leucopus* is the higher baseline expression of some ISGs as noted here (Figure 9 and Figure S6).

Reducing differences between *P. leucopus* and murids *M. musculus* and *R. norvegicus* to a single attribute, such as the documented inactivation of the Fcgr1 gene in *P. leucopus* [7], may be fruitless. But the feature that may best distinguish the deermouse from the mouse and rat is its predominantly anti-inflammatory quality. This characteristic likely has a complex, polygenic basis, with environmental (including microbiota) and epigenetic influences. An individual's placement is on a spectrum or, more likely, a landscape rather than in one or another binary or Mendelian category.

One argument against a purely anti-inflammatory characterization is the greater neutrophil numbers and activity in *P. leucopus* compared to *M. musculus* in the LPS experiment. The neutrophil activation, migration, and phagocytosis would be appropriate early defenses against a pyogenic pathogen. But if not contained, they bring local and systemic risks for the host. This damage would not likely be from nitric oxide and reactive nitrogen species, given the minimal Nos2 transcription. But deermice showed heightened expression of proteases, such as Mmp8, enzymes for reactive oxygen species, such as NADPH oxidase 1 (Nox1), and facilitators of neutrophil extracellular traps, such as PAD4 (Padi4) (Table 2). We had previously identified possible mitigators, such as the protease inhibitor Slpi and superoxide dismutase 2 [3]. These findings were replicated here. The topic of neutrophil activation and these and other possible counters is considered in more detail elsewhere.

An anti-inflammatory disposition but at what cost?

An assignment of infection tolerance to a host and pathogen pairing assumes sufficient immunity against the microbe to keep it in check if elimination fails. *P. leucopus* and *P. maniculatus*, are in this sense "immunocompetent" with respect to the microbes they host and with which they may share a long history [40]. Yet, has this balance of resistance and tolerance for certain host-associated microbes been achieved in a trade-off that entails vulnerabilities to other types of agents?

The selection of LPS as the experimental model was meant to cover this contingency, at least for the common denominator of acute inflammation many types of infections elicit. But LPS studies revealed potential weaknesses that some pathogens might exploit. One of these is the low expression of inducible nitric oxide. Although Nos2 gene knockouts in *M. musculus* had lower LPS-induced mortality than their wild-type counterparts, the mutants were more susceptible to the protozoan *Leishmania major* and the facultative intracellular bacterium *Listeria monocytogenes* [56, 93]. While

there are no known studies of either of these pathogens in *P. leucopus*, the related species *P. yucatanicus* is the main reservoir for *Leishmania mexicana* in Mexico [17]. Compared with *M. musculus*, which suffer a high fatality rate from experimental infections with *L. mexicana*, *P. yucatanicus* infections are commonly asymptomatic [54].

Given the restrained interferon and ISG response shown by *P. leucopus*, another plausible vulnerability would be viral infections. But other studies suggest that neither RNA nor DNA viruses pose an inordinately high risk for *Peromyscus*. Both tolerance of and resistance to the tickborne encephalitis flavivirus Powassan virus by *P. leucopus* were demonstrated in an experimental model in which mice, by contrast ,were severely affected [62]. *P. maniculatus* has been successfully infected with the SARS-CoV-2 virus by the respiratory route, but the infected animals displayed only mild pathology, manifested little if any disability, and recovered within a few days [30, 33]. Among natural populations and in the laboratory *P. maniculatus* is noted for its tolerance of hantavirus, which commonly is fatal for infected humans [14, 20]. *P. maniculatus* was permissive of infection with monkeypox virus, but the infection was mild and transient [26].

A distinguishing *P. leucopus* characteristic, which was not expressly examined here, is its aforementioned 2-3 fold greater life span than that of *M. musculus*. While deermice may not be in the same longevity league as the naked mole-rat (*Heterocephalus glaber*), which can live for over 30 years [73], some features of naked mole-rat immunology are intriguingly similar to what we have observed for *P. leucopus*. These include macrophages and blood myeloid cells with low to absent transcription of Nos2 or production of nitric oxide in response to LPS, even in the presence of added inteferon-gamma [31]. Like *P. leucopus* and in distinction to *M. musculus*, naked mole-rats showed an increase in the proportion of neutrophils in the blood 4 hours after intraperitoneal injection of LPS [39]. In another comparative study, the hematopoietic stem and progenitor cells of these rodents had a lower type 1 interferon response than mice to a TLR3 agonist [28].

In summary, if there is a vulnerability that *Peromyscus* accepts in return for relief from inflammation (and perhaps a longer life), it has not been identified yet. However, potential threats and stressors are many, and the number assessed either in the field or laboratory has been limited to date.

Implications for Lyme disease and other zoonoses

Our studies of *P. leucopus* began with a natural population and documented a >80% prevalence of infection and high incidence of re-infections by *B. burgdorferi* in the area's white-footed deermouse, the most abundant mammal there [16]. This was a Lyme disease endemic area [27], where residents frequently presented for medical care for a variety of clinical manifestations, from mild to serious, of *B. burgdorferi* infection [85]. Subclinical infections in humans occur, but most of those who become infected have a definable illness [86]. The localized or systemic presence of the microbe is a necessary condition for Lyme disease, but the majority of the symptoms and signs are attributable to inflammation elicited by the organism's presence and not from virulence properties per se or the hijacking of host cells [21]. Since humans are transmission dead-ends for *B. burgdorferi* and many other zoonotic agents in their life cycles, it is not surprising that human infections are generally more debilitating if not fatal than what adapted natural hosts experience.

It is in the space between the asymptomatic natural host and symptomatic inadvertent host where there may be insights with basic and translational application. With this goal, we consider the ways the results inform studies of the pathogenesis of Lyme disease, where "disease" includes lingering disorders akin to "long Covid" [71], and where "pathogenesis" includes both microbial and host contributions. Plausibly-germane deermouse-mouse differences identified in our studies are summarized in Figure 11. Two are highlighted here.

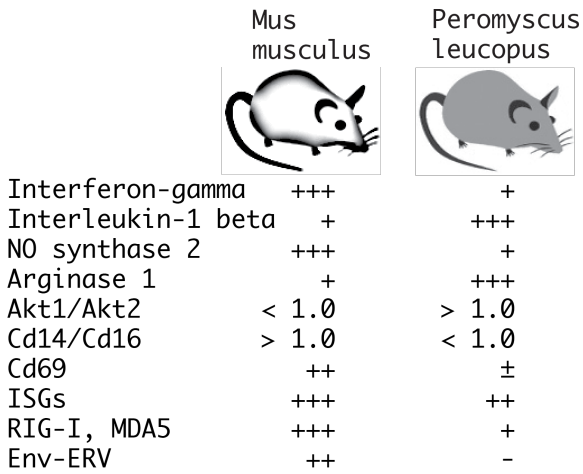

Figure 11. Summary of distinguishing features of transcriptional responses in the blood between *P. leucopus* and *M. musculus* 4 h after treatment with LPS. There is semi-quantitative representation of relative transcription of selected coding sequences or ratios of transcription for selected pairs of genes in the blood.

The first is macrophage polarization [68]. By the criteria summarized above, the response to LPS by *P. leucopus* is consistent with the alternatively-activated or M2 type, rather than the expected classical or M1 type. But it was not only LPS-treated deermice that had this attribute, the blood of untreated animals also displayed M2 type polarization features. This included a comparatively high Arg1 expression level and a Akt1/Akt2 ratio of more than 1 at baseline. This suggests that studies of other mammals, including humans, need not administer LPS or other TLR agonist to assess disposition toward M1 or M2-type polarization. This reading could serve as a prognostic indicator of the inflammatory response to infection with *B. burgdorferi* or other pathogen and the long-term outcome.

The second difference we highlight is the activation of ERV transcription that was prominent in the LPS-treated mice and rats but not in similarly-treated deermice. A paradoxical enlistment of antiviral defenses, including type 1 and type 2 interferons, for an infection with an extracellular bacterium, like *B. burgdorferi*, may bring about more harm than benefit, especially if the resultant inflammation persists after antibiotic therapy. There are various ways to assess ERV activation in the blood, including assays for RNA, protein, and reverse transcriptase activity. A xenotropic MLV-related retrovirus has been discounted as a cause of chronic fatigue syndrome [60]. However, production of whole virions need not occur for there to be PRR signaling in response to cytoplasmic Env protein, single stranded RNA, or cDNA [78].

METHODS

Animals

The study was carried out in accordance with the *Guide for the Care and Use of Laboratory Animals: Eighth Edition* of the National Academy of Sciences. The protocols AUP-18-020 and AUP-21-007 were approved by the Institutional Animal Care and Use Committee of the University of California Irvine.

Peromyscus leucopus, here also referred to as "deermice", were of the outbred LL stock, which originated with 38 animals captured near Linville, NC and thereafter comprised a closed colony without sib-sib matings at the *Peromyscus* Genetic Stock Center at the University of South Carolina [45]. The LL stock animals for this study were bred and raised at the vivarium of University of California Irvine, an AAALAC approved facility. Outbred *Mus musculus* breed CD-1, specifically Crl:CD1(ICR) IGS, and here also referred to as "mice", were obtained from Charles River. Fischer F344 strain inbred *Rattus norvegicus*, specifically F344/NHsd, and here also referred to as "rats", were obtained from Charles River.

For the combined *P. leucopus-M. musculus* experiment the 20 *P. leucopus* were of a mean (95% confidence interval) 158 (156-159) days of age and had a mean 21 (19-22) g body mass. The 20 *M. musculus* were all 149 days of age and had a mean body mass of 47 (43-50) g. The ratio of average male to average female body mass was 1.04 for *P. leucopus* and 1.03 for *M. musculus*. The 6 female *P. leucopus* for the 12 h duration experiment were of a mean 401 (266-535) days of age and mean body mass of 20 (17-23) g. The 16 adult 10-12 week old female *R. norvegicus* had a mean 139 (137-141) g body mass. The 7 male *P. leucopus* for the infection study were of a mean 107 (80-134) days and mean body mass of 21 (18-24) g.

Animals were housed in Techniplast-ventilated cages in vivarium rooms with a 16 h-8 h light-dark cycle, an ambient temperature of 22 °C, and on ad libitum water and a diet of 2020X Teklad global soy protein-free extruded rodent chow with 6% fat content (Envigo, Placentia, CA).

For injections the rodents were anesthetized with inhaled isoflurane. The rodents were euthanized by carbon dioxide overdose and intracardiac exsanguination at the termination of the experiment. No animals died or became moribund before the 4 hour or 12 h termination time points in the LPS experiments or before the 5 d termination point of infection study.

LPS experiments

For the *P. leucopus* and *M. musculus* combined experiment, sample sizes replicated the specifications of the previous study, in which there were 20 *P. leucopus* and 20 *M. musculus*, equally divided between females and males and equally allotted between conditions [3]. The treatments were administered in the morning of a single day. At 15 min intervals and alternating between species, sex, and treatments, animals were intraperitoneally (ip) injected 50 µl volumes of either ion-exchange chromatography-purified *Escherichia coli* O111:B4 LPS (Sigma-Aldrich L3024) in a dose of 10 µg per g body mass or the diluent alone: sterile-filtered, endotoxin-tested, 0.9% sodium chloride (Sigma-Aldrich). The animals were visually monitored in separate cages continuously for the duration of the experiment. We recorded whether there was reduced activity by criterion of huddling with little or movement for > 5 min, ruffled fur or piloerection), or rapid respiration rate or tachypnea. At 4.0 h time after injection animals were euthanized as described above, and sterile dissection was carried out immediately.

Lower dose and longer duration experiment. In an experiment with 6 *P. leucopus*, the animals were administered the same single dose of LPS but at 1.0 µg/g and the same control solution. The animals were euthanized 12 h after the injection the following day.

Rat LPS experiment. The same experimental design was used for the rats as for the combined deermice-mice experiment, with the exception that the formulation of the *E. coli* O111:B4 LPS was "cell culture grade" (Sigma-Aldrich L4391), and the groups were sterile saline alone (n = 5), 5 µg LPS per g body mass (n = 6), or 20 µg LPS per g (n = 5).

Experimental infection

The infection of a group of *P. leucopus* LL stock with the relapsing fever agent *B. hermsii* and the processing of blood and tissues for RNA extraction 5 days into the infection were described previously [3]. In brief, animals were infected intraperitoneally on day 0 with either phosphate-buffered saline alone or 10^3 cells of *B. hermsii* MTW, a strain that is infectious for *Peromyscus* species [43]. Bacteremia was confirmed by microscopy on day 4, and the animals were euthanized on day 5. For that prior study the RNA-seq analysis was limited to the genome-wide transcript reference set. For the present study we used the original fastq format files for targeted RNA-seq as described below.

Hematology and plasma analyte assays

For the combined *P. leucopus-M. musculus* experiment automated complete blood counts with differentials were performed at Antech Diagnostics, Fountain Valley, CA on a Siemens ADVIA 2120i with Autoslide hematology instrument with manual review of blood smears by a veterinary pathologist. For the 12 h duration *P. leucopus* experiment hematologic parameters were analyzed on an ABCVet Hemalyzer automated cell counter instrument at U.C. Irvine. For the rat experiment complete blood counts with differentials were performed at the Comparative Pathology Laboratory

of the University of California Davis. Multiplex bead-based cytokine protein assay of the plasma of the rats was performed at Charles River Laboratories using selected options of the Millipore MILLIPLEX MAP rat cytokine/chemokine panel.

RNA extraction of blood

After the chest cavity was exposed, cardiac puncture was performed through a 25 gauge needle into a sterile 1 ml polypropylene syringe. After the needle was removed, the blood was expelled into Becton-Dickinson K2E Microtainer Tubes, which contained potassium EDTA. Anticoagulated blood was split into a sample that was placed on ice for same-day delivery to the veterinary hematology laboratory and a sample intended for RNA extraction which was transferred to an Invitrogen RiboPure tube with DNA/RNA Later and this suspension was stored at -20 °C. RNA was isolated using the Invitrogen Mouse RiboPure-Blood RNA Isolation Kit]. RNA concentration was determined on a NanoDrop microvolume spectrophotometer (ThermoFisher) and quality was assessed on an Agilent Bioanalyzer 2100.

RNA-seq of blood

The chosen sample sizes and coverage for the bulk RNA-seq were based on empirical data from the prior study [3], which indicated that with 10 animals per group and a two-sided two sample *t*-test we could detect with a power of ≥ 0.80 and at a significance level of 0.05 a ≥1.5 fold difference in transcription between groups for a given gene. We also were guided by the simulations calculations of Hart et al. [36], which indicated for a biological coefficient of variation of 0.4 within a group, a minimum depth of coverage of ≥ 10, and a target of ≥ 2x fold change that a sample size of 7-8 was sufficient for 80% power and type I error of 5%. For the *P. leucopus* and *M. musculus* samples production of cDNA libraries was with the Illumina TruSeq Stranded mRNA kit. After normalization and multiplexing, the libraries were sequenced at the University of California Irvine's Genomic High Throughput Facility on a Illumina NovaSeq 6000 instrument with paired-end chemistry and 150 cycles to achieve ~100 million reads per sample for the combined *P. leucopus-M. musculus* experiment. The same method for producing cDNA libraries was used for the *R. norvegicus* RNA and the *P. leucopus* in the infection study, but these were sequenced on a Illumina HiSeq 4000 instrument with paired-end chemistry and 100 cycles. The quality of sequencing reads was analyzed using FastQC (Babraham Bioinformatics). The reads were trimmed of low-quality reads (Phred score of <15) and adapter sequences, and corrected for poor-quality bases using Trimmomatic [12].

For the combined species experiment the mean (95% CI) number of PE150 reads per animal after trimming for quality was 1.1 (1.0-1.2) x 10^8 for *P. leucopus* and 1.1 (1.0-1.2) x 10^8 for *M. musculus* (p = 0.91). For *P. leucopus* of this experiment a mean of 83% of the reads mapped to the genome transcript reference set of 54,466; mean coverages for all transcripts and for the mean 62% of reference transcripts with ≥ 1x coverage were 97x and 157x, respectively. For *M. musculus* of this experiment a mean 91% of the reads mapped to the genome transcript reference set of 130,329; mean coverages for all transcripts and for the mean of 21% of reference transcripts with ≥ 1x coverage were 103x and 568x, respectively. For the lower dose-longer duration experiment with *P. leucopus* the mean number of PE150 reads was 2.5 (2.3-2.6) x 10^7. For the rat experiment the mean number of PE100 reads was 2.4 (2.2-2.5) x 10^7. For the *B. hermsii* infection experiment the mean number of PE100 reads was 4.9 (4.5-5.3) x 10^7.

Batched fastq files were subjected to analysis with CLC Genomics Workbench version 23 (Qiagen). Library size normalization was done by the TMM (trimmed mean of M values) method of Robinson and Oshlack [77]. The reference genome transcript sets on GenBank were the following: GCF_004664715.2 for *P. leucopus* LL stock, GCF_000001635.27_GRCm39 for *M. musculus* C57Bl/6, and GCF_015227675.2_mRatBN7.2 for *R. norvegicus*. The settings for PE150 reads were as follows for both strands: length fraction of 0.35, similarity fraction of 0.9, and costs for mismatch, insertion, or deletion of 3. For PE100 reads the settings were the same except for length fraction of 0.4. Principal Component Analysis was carried with the "PCA for RNA-Seq" module of the suite of programs.

For the *P. leucopus* RNA-seq analysis there were 54,466 reference transcripts, of which 48,164 (88%) were mRNAs with protein coding sequences, and 6,302 were identified as non-coding RNAs (ncRNA). Of the 48,164 coding sequences, 40,247 (84%) had matching reads for at least one of the samples. The five most highly represented *P. leucopus* coding sequences among the matched transcripts of whole blood among treated and control animals were hemoglobin subunits alpha and beta, the calprotectin subunits S100A8 and S100A9, and ferritin heavy chain. For the *M. musculus* analysis there were available 130,329 reference transcripts: 92,486 (71%) mRNAs with protein coding sequences and 37,843 ncRNAs. Of the coding sequences, 59,239 (64%) were detectably transcribed in one or both groups by the same criterion. The five most highly represented coding sequences of mRNAs of identified genes for *M. musculus* were hemoglobin subunits alpha and beta, aminolevulinic synthase 2, ferritin light polypeptide 1, and thymosin beta. For *R. norvegicus* there were 99,126 reference transcripts, of which 74,742 (75%) were mRNAs. The five most highly represented coding sequences of mRNAs of identified genes for *R. norvegicus* were hemoglobin subunits alpha and beta, beta-2 microglobulin, ferritin heavy chain, and S100a9.

Genome-wide differential gene expression

Differential expression between experimental conditions was assessed with an assumption of a negative binomial distribution for expression level and a separate Generalized Linear Model for each [59]. Fold changes in TPM (transcripts per million) were $\log_2$-transformed. The False Discovery Rate (FDR) with corrected *p* value was estimated by the method of Benjamini and Hochberg [10]. To assess the limit of detection for differentially expressed genes between 10 animals treated with LPS and 10 with saline alone, we took the data for 4650 reference transcripts for which the mean TPM across 20 *P. leucopus* was >10 and randomly permuted the data to achieve another 9 sets and calculated the fold-change of sub-groups of 10 and 10 with one random group serving as the proxy of the experimental treatment and other second as the control for each of the sets. The expectation was that mean fold-change of the 9 permuted sets and the 4650 reference sequences would be ~1. The result was a mean and median of 1.08 with a 99.9% asymmetric confidence interval for the mean of 0.81-1.49. This was an indication that the choices for sample sizes were realistic for achieving detection of ≥ 1.5x fold changes.

Gene Ontology term analysis

M. musculus was selected as the closest reference for the *P. leucopus* data. The analysis was implemented for data for differentially expressed genes meeting the criteria of a FDR *p*-value ≤ 0.01 and fold-change of ≥ 1.5. The analysis was implemented with the tools of Metascape (https://metascape.org) [99]. Functional enrichment analysis was carried out first with the hypergeometric test and FDR *p*-value correction [10]. Then pairwise similarities between any two enriched terms were computed based on a Kappa-test score [22]. Similarity matrices were then hierarchically clustered and a 0.3 similarity threshold was applied to trim resultant trees into separate clusters. The lower the *p*-value, the less the likelihood the observed enrichment is due to randomness [98]. The lowest *p*-value term represented each cluster shown in the horizontal bar graph. Besides the terms beginning with "GO" and referring to the Gene Ontology resource (http://geneontology.org) [2], others refer to Kegg Pathway database (https://www.kegg.jp) for "mmu.." designations, WikiPathways database (https://www.wikipathways.org) for "WP…" designations, and Reactome database (https://reactome.org) for "R-MMU…" designations.

Targeted RNA-seq

RNA-seq of selected set of protein coding sequences (CDS), which are listed below, was carried out using CLC Genomics Workbench v. 23 (Qiagen). Paired-end reads were mapped with a length fraction of 0.35 for ~150 nt reads and 0.40 for ~100 nt reads, a similarity fraction of 0.9, and costs of 3 for mismatch, insertion, or deletion to the CDS of sets of corresponding orthologous mRNAs of *P. leucopus*, *M. musculus*, and *R. norvegicus*. Preliminary expression values were unique reads normalized for total reads across all the samples without adjustment for reference sequence length, as described [3]. Exceptions were the endogenous retrovirus coding sequences which differed in lengths between species. For within- and cross-species comparisons we initially normalized three

different ways after quality filtering and removing vector and linker sequence: for total reads for the given sample, for unique reads for 12S ribosomal RNA for the mitochondria of nucleated cells in the blood, and for unique reads for the gene Ptprc, which encodes CD45, a marker for both granulocytes and mononuclear cells in the blood. This is described in more detail in Results. Following the recommendation of Hedges et al. we used the natural logarithm (*ln*) of ratios [37].

The target CDS were as follows: Acod1, Akt1, Akt2, Arg1, Bcl3, Camp, Ccl2, Ccl3, Ccl4, Cd14, Cd177, Cd3d, Cd4, Cd69, Cd8, Cfb, Cgas, Csf1, Csf1r, Csf2, Csf3, Csf3r, Cx3cr1, Cxcl1, Cxcl10, Cxcl2, Cxcl3, Dhx58, Fcer2, Fcgr2a, Fcgr2b, Fcgr3 (CD16), Fgr, Fos, Fpr2, Gapdh, Gbp4, Glrx, Gzmb, Hif1a, Hk3, Hmox1, Ibsp, Icam, Ifih1, Ifit1, Ifng, Il10, Il12, Il18, Il1b, Il1rn, Il2ra, Il4ra, Il6, Il7r, Irf7, Isg15, Itgam, Jak1, Jak2, Jun, Lcn2, Lpo, Lrg, Lrrk2, Ltf, Mapk1, Mmp8, Mmp9, Mpo, MT-Co1, Mt2, Mtor, Mx2, Myc, Myd88, Ncf4, Nfkb1, Ngp, Nos2, Nox1, Nr3c1, Oas1, Olfm4, Padi4, Pbib, Pkm, Ptx, Ptprc (CD45), Retn, Rigi (Ddx58), S100a9, Saa3, Serpine1, Slc11a1 (Nramp), Slpi, Socs1, Socs3, Sod2, Stat1, Stat2, Stat4, Steap1, Sting, Tgfb, Thy1, Timp1, Tlr1, Tlr2, Tlr4, Tnf, Tnfrsf1a, and Tnfrsf9. The sources for these coding sequences were the reference genome transcript sets for *P. leucopus, M. musculus*, and *R. norvegicus* listed above. If there were two or more isoforms of the mRNAs and the amino acid sequences differed, the default selection for the coding sequence was the first listed isoform. The lengths of the orthologous pairs of *P. leucopus* and *M. musculus* coding sequences were either identical or within 2% of the other. Fcgr1, the gene for high affinity Fc gamma receptor I or CD64, was not included in the comparison, because in *P. leucopus* it is an untranscribed pseudogene [7]. For the targeted RNA-seq of blood of deermice infected with *B. hermsii* (Table 6), the reference sequence was the cp6.5 plasmid of *B. hermsii* (NZ_CP015335).

Quantitative PCR assays

Reverse transcriptase (RT)-qPCR assays and the corresponding primers for measurement of transcripts of genes for nitric oxide synthase 2 (Nos2) and glyceraldehyde 3-phosphate dehydrogenase (Gapdh) were those described previously [3]. These primers worked for *M. musculus* as well as *P. leucopus* using modified cycling conditions. For the arginase 1 transcript assays different primer sets were used for each species. The forward and reverse primer sets for the 352 bp Arg1 product for *P. leucopus* were 5'-TCCGCTGACAACCAACTCTG and 5'-GACAGGTGTGCCAGTAGATG, respectively. The corresponding primer pairs for a 348 bp Arg1 of *M. musculus* were 5'-TGTGAAGAACCCACGGTCTG and 5'-ACGTCTCGCAAGCCAATGTA. cDNA synthesis and qPCR were achieved with a Power Sybr Green RNA-to-Ct 1-Step Kit (Applied Biosystems) in 96 MicroAmp Fast Reaction Tubes using an Applied Biosystems StepOne Plus real-time PCR instrument. The initial steps for all assays were 48 °C for 30 min and 95 °C for 10 min. For Arg1 and Nos2 assays, this was followed by 40 cycles of a 2-step PCR of, first, 95°C for 15 s and then, second, annealing and extension at 60 °C for 1 min. The cycling conditions for Gapdh were 40 cycles of 95 °C for 15 s followed by 60 °C for 30 s. Quantitation of genome copies of *B. hermsii* in extracted DNA was carried out by probe-based qPCR as described [6].

Additional statistics

Means are presented with asymmetrical 95% confidence intervals (CI) to accommodate data that was not normally distributed. Parametric (*t* test) and non-parametric (Mann-Whitney) tests of significance were 2-tailed. Unless otherwise stated, the *t* test *p* value is given. Categorical variables were assessed by 2-tailed Fisher's exact test. FDR correction of *p* values for multiple testing was by the Benjamini-Hochberg method [10], as implemented in CLC Genomics Workbench (see above), or False Discovery Rate Online Calculator (https://tools.carbocation.com/FDR). Discriminant Analysis, linear regression, correlation, coefficient of determination, and General Linear Model analyses were performed with SYSTAT v. 13.1 software (Systat Software, Inc.). Box plots with whiskers display the minimum, first quartile, median, third quartile, and maximum.

Data availability

The experiments reported here are associated with National Center for Biotechnology Information (https://ncbi.nlm.nih.gov) BioProjects PRJNA975149 for the combined *P. leucopus* and *M. musculus* experiment, PRJNA874306 for the 12 h-lower dose *P. leucopus* experiment,

PRJNA973677 for the *R. norvegicus* LPS experiment, and PRJNA508222 for the *B. hermsii* infection of *P. leucopus* experiment. PRJNA975149 includes 40 BioSamples (SAMN35347136-SAMN35347175) and 40 sets of Sequence Read Archive (SRA) fastq files of Illumina paired-end chemistry reads 1 and 2 (SRR24733648-SRR24733687). PRJNA874306 includes 6 BioSamples (SAMN30561752-SAMN30561757) and the corresponding SRA files SRR24451178-SRR24451180, SRR24451183, SRR24451194, and SRR24451195. PRJNA973677 includes 16 BioSamples (SAMN35351370-SAMN35351385) and the corresponding SRA files SRR24731678- SRR24731693. PRJNA508222 includes 7 BioSamples (SAMN10522571- SAMN10522573; SAMN10522575-SAMN10522578) and SRA files (SRR8283809; SRR8283811-SRR8283816). The datasets of the genome-wide RNA-seq and the differentially-expressed gene analysis of RNA-seq data for the 4 h LPS experiments for *P. leucopus*, *M. musculus*, and *R. norvegicus* are available under the title "Differentially-expressed genes in blood in response to lipopolysaccharide in three rodent species" at the public data repository Dryad (https://datadryad.org). The link for Dryad Tables D1-D6 and their descriptions is https://doi.org/10.5061/dryad.zw3r228dh. A Transcriptome Shotgun Assembly (TSA) for stranded mRNA of blood of the 20 female and male *P. leucopus* of the 4 h LPS experiment comprised 14,982 contigs of ≥ 400 nt and ≥ 20x coverage and have TSA accession number GKOE00000000.

Acknowledgments

We thank Hanjuan Shao for technical assistance, Vanessa Cook for her participation in the *R. norvegicus* experiment, Anthony Long for bioinformatic advice and contributions, and Brianna Craver-Hoover and Gajalakshmi Ramanathan for assistance with blood cell counts performed at U.C. Irvine. The experimental studies reported here were supported by National Institutes of Health (NIH) grants AI-157513 and AI-136523. The services of the Genomics Research and Technology Hub were administratively supported in part by NIH Cancer Center Support Grant P30 CA-062203 and NIH shared instrumentation grants RR-025496, OD-010794, and OD-021718.

REFERENCES

1. Arranz A, Doxaki C, Vergadi E, Martinez de la Torre Y, Vaporidi K, Lagoudaki ED, Ieronymaki E, Androulidaki A, Venihaki M, Margioris AN. Akt1 and Akt2 protein kinases differentially contribute to macrophage polarization. Proc Natl Acad Sci U S A. 2012;109(24):9517-22.
2. Ashburner M, Ball CA, Blake JA, Botstein D, Butler H, Cherry JM, Davis AP, Dolinski K, Dwight SS, Eppig JT, Harris MA, Hill DP, Issel-Tarver L, Kasarskis A, Lewis S, Matese JC, Richardson JE, Ringwald M, Rubin GM, Sherlock G. Gene Ontology: tool for the unification of biology. Nature Genet. 2000;25(1):25-9. doi: 10.1038/75556.
3. Balderrama-Gutierrez G, Milovic A, Cook VJ, Islam MN, Zhang Y, Kiaris H, Belisle JT, Mortazavi A, Barbour AG. An infection-tolerant mammalian reservoir for several zoonotic agents broadly counters the inflammatory effects of endotoxin. mBio. 2021;12(2). Epub 20210413. doi: 10.1128/mBio.00588-21. PMCID: PMC8092257.
4. Barbour AG. Infection resistance and tolerance in Peromyscus spp., natural reservoirs of microbes that are virulent for humans. Semin Cell Devel Biol. 2017;61(1):115-22. doi: 10.1016/j.semcdb.2016.07.002. PMCID: PMC5205561.
5. Barbour AG. *Borreliaceae*. In: Whitman WB, Rainey R, P. Kämpfe P, Trujillo M, Chun J, DeVos P, Hedlund B, Dedysh S, editors. *Bergey's Manual of Systematics of Archaea and Bacteria*. 2018. p. 1-9. Wiley, Hoboken, NJ, USA
6. Barbour AG, Bunikis J, Travinsky B, Hoen AG, Diuk-Wasser MA, Fish D, Tsao JI. Niche partitioning of Borrelia burgdorferi and Borrelia miyamotoi in the same tick vector and mammalian reservoir species. Am J Trop Med Hyg. 2009;81(6):1120-31. doi: 10.4269/ajtmh.2009.09-0208. PMCID: PMC2841027.

7. Barbour AG, Duong JV, Long AD. Lyme disease agent reservoirs *Peromyscus leucopus* and *P. maniculatus* have natively inactivated genes for the High-Affinity Immunoglobulin Gamma Fc Receptor I (CD64). Pathogens. 2023;12(8):1056. doi: 10.3390/pathogens12081056.
8. Bashirova AA, Apps R, Vince N, Mochalova Y, Yu XG, Carrington M. Diversity of the human LILRB3/A6 locus encoding a myeloid inhibitory and activating receptor pair. Immunogenetics. 2014;66(1):1-8. doi: 10.1007/s00251-013-0730-9. PMCID: PMC3877738.
9. Bedford NL, Hoekstra HE. Peromyscus mice as a model for studying natural variation. eLife. 2015;4:e06813. doi: 10.7554/eLife.06813. PMCID: PMC4470249.
10. Benjamini Y, Hochberg Y. Controlling the false discovery rate: a practical and powerful approach to multiple testing. J Roy Stat Soci Series B (Methodological). 1995;57(1):289-300. doi: 10.1111/j.2517-6161.1995.tb02031.x.
11. Biser JA, Vogel LA, Berger J, Hjelle B, Loew SS. Effects of heavy metals on immunocompetence of white-footed mice (Peromyscus leucopus). J Wildl Dis. 2004;40(2):173-84. doi: 10.7589/0090-3558-40.2.173. PubMed PMID: 15362816.
12. Bolger AM, Lohse M, Usadel B. Trimmomatic: a flexible trimmer for Illumina sequence data. Bioinformatics. 2014;30(15):2114-20. doi: 10.1093/bioinformatics/btu170. PMCID: PMC4103590.
13. Bothwell A, Pace PE, LeClair KP. Isolation and expression of an IFN-responsive Ly-6C chromosomal gene. J Immunol. 1988;140(8):2815-20. PubMed PMID: 3356904.
14. Botten J, Mirowsky K, Kusewitt D, Bharadwaj M, Yee J, Ricci R, Feddersen RM, Hjelle B. Experimental infection model for Sin Nombre hantavirus in the deer mouse (Peromyscus maniculatus). Proc Natl Acad Sci U S A. 2000;97(19):10578-83. doi: 10.1073/pnas.180197197. PMCID: Pmc27067.
15. Bradley RD, Ammerman LK, Baker RJ, Bradley LC, Cook JA, Dowler RC, Jones C, Schmidly DJ, Stangl FB, Van Den Bussche RA. Revised checklist of North American mammals north of Mexico, 2014: Museum of Texas Tech University; 2014. https://www.depts.ttu.edu/nsrl/publications/downloads/OP327.pdf
16. Bunikis J, Tsao J, Luke CJ, Luna MG, Fish D, Barbour AG. Borrelia burgdorferi infection in a natural population of Peromyscus leucopus mice: a longitudinal study in an area where Lyme Borreliosis is highly endemic. J Infect Dis. 2004;189(8):1515-23. doi: 10.1086/382594
17. Chable-Santos JB, Van Wynsberghe NR, Canto-Lara SB, Andrade-Narvaez FJ. Isolation of Leishmania (L.) mexicana from wild rodents and their possible role in the transmission of localized cutaneous leishmaniasis in the state of Campeche, Mexico. Am J Trop Med Hyg. 1995;53(2):141-5. doi: 10.4269/ajtmh.1995.53.141. PubMed PMID: 7677214.
18. CharlesRiver. CD-1 Mouse Hematology: Charles River; 2012 [cited 2023 March 30, 2023]. Available from: https://www.criver.com/sites/default/files/resources/doc_a/CD-1MouseClinicalPathologyData.pdf.
19. Chiaranunt P, Burrows K, Ngai L, Cao EY, Liang H, Tai SL, Streutker CJ, Girardin SE, Mortha A. NLRP1B and NLRP3 Control the host response following colonization with the commensal protist Tritrichomonas musculis. J Immunol. 2022;208(7):1782-9. doi: 10.4049/jimmunol.2100802.
20. Childs JE, Ksiazek TG, Spiropoulou CF, Krebs JW, Morzunov S, Maupin GO, Gage KL, Rollin PE, Sarisky J, Enscore RE, et al. Serologic and genetic identification of Peromyscus maniculatus as the primary rodent reservoir for a new hantavirus in the southwestern United States. J Infect Dis. 1994;169(6):1271-80. PubMed PMID: 8195603.
21. Coburn J, Garcia B, Hu LT, Jewett MW, Kraiczy P, Norris SJ, Skare J. Lyme disease pathogenesis. Curr Issues Molec Biol. 2021;42(1):473-518.
22. Cohen J. A coefficient of agreement for nominal scales. Educational and Psychological Measurement. 1960;20(1):37-46.

23. Cook V, Barbour AG. Broad diversity of host responses of the white-footed mouse Peromyscus leucopus to Borrelia infection and antigens. Ticks Tick Borne Dis. 2015;6(5):549-58. Epub 2015/05/26. doi: 10.1016/j.ttbdis.2015.04.009. PMCID: PMC4504778.
24. Crowder CD, Ghalyanchi Langeroudi A, Shojaee Estabragh A, Lewis ER, Marcsisin RA, Barbour AG. Pathogen and host response dynamics in a mouse model of Borrelia hermsii relapsing fever. Vet Sci. 2016;3(3):19. doi: 10.3390/vetsci3030019.
25. De Cecco M, Ito T, Petrashen AP, Elias AE, Skvir NJ, Criscione SW, Caligiana A, Brocculi G, Adney EM, Boeke JD, Le O, Beauséjour C, Ambati J, Ambati K, Simon M, Seluanov A, Gorbunova V, Slagboom PE, Helfand SL, Neretti N, Sedivy JM. L1 drives IFN in senescent cells and promotes age-associated inflammation. Nature. 2019;566(7742):73-8. doi: 10.1038/s41586-018-0784-9.
26. Deschambault Y, Klassen L, Soule G, Tierney K, Azaransky K, Sloan A, Safronetz D. Experimental infection of North American Deer Mice with Clade I and II Monkeypox Virus Isolates. Emerg Infect Dis. 2023;29(4):858-60. Epub 20230306. doi: 10.3201/eid2904.221594. PMCID: PMC10045688.
27. Diuk-Wasser MA, Hoen AG, Cislo P, Brinkerhoff R, Hamer SA, Rowland M, Cortinas R, Vourc'h G, Melton F, Hickling GJ, Tsao JI, Bunikis J, Barbour AG, Kitron U, Piesman J, Fish D. Human risk of infection with Borrelia burgdorferi, the Lyme disease agent, in eastern United States. Am J Tropl Med Hyg. 2012;86(2):320-7. doi: 10.4269/ajtmh.2012.11-0395. PMCID: PMC3269287.
28. Emmrich S, Trapp A, Tolibzoda Zakusilo F, Straight ME, Ying AK, Tyshkovskiy A, Mariotti M, Gray S, Zhang Z, Drage MG, Takasugi M, Klusmann JH, Gladyshev VN, Seluanov A, Gorbunova V. Characterization of naked mole-rat hematopoiesis reveals unique stem and progenitor cell patterns and neotenic traits. EMBO J. 2022;41(15):e109694. doi: 10.15252/embj.2021109694. PMCID: PMC9340489.
29. Escalante NK, Lemire P, Cruz Tleugabulova M, Prescott D, Mortha A, Streutker CJ, Girardin SE, Philpott DJ, Mallevaey T. The common mouse protozoa Tritrichomonas muris alters mucosal T cell homeostasis and colitis susceptibility. J Exp Med. 2016;213(13):2841-50. doi: 10.1084/jem.20161776. PMCID: PMC5154950.
30. Fagre A, Lewis J, Eckley M, Zhan S, Rocha SM, Sexton NR, Burke B, Geiss B, Peersen O, Bass T, Kading R, Rovnak J, Ebel GD, Tjalkens RB, Aboellail T, Schountz T. SARS-CoV-2 infection, neuropathogenesis and transmission among deer mice: implications for spillback to New World rodents. PLoS Pathogens. 2021;17(5):e1009585. doi: 10.1371/journal.ppat.1009585. PMCID: PMC8168874.
31. Gorshkova EA, Gubernatorova EO, Dvorianinova EM, Yurakova TR, Marey MV, Averina OA, Holtze S, Hildebrandt TB, Dmitriev AA, Drutskaya MS, Vyssokikh MY, Nedospasov SA. Macrophages from naked mole-rat possess distinct immunometabolic signatures upon polarization. Front Immunol. 2023;14:1172467. doi: 10.3389/fimmu.2023.1172467. PMCID: PMC10154529.
32. Gozashti L, Feschotte C, Hoekstra HE. Transposable element interactions shape the ecology of the deer mouse genome. Mol Biol Evol. 2023;40(4):msad069. doi: 10.1093/molbev/msad069; PMCID: PMC10089650.
33. Griffin BD, Chan M, Tailor N, Mendoza EJ, Leung A, Warner BM, Duggan AT, Moffat E, He S, Garnett L, Tran KN, Banadyga L, Albietz A, Tierney K, Audet J, Bello A, Vendramelli R, Boese AS, Fernando L, Lindsay LR, Jardine CM, Wood H, Poliquin G, Strong JE, Drebot M, Safronetz D, Embury-Hyatt C, Kobasa D. SARS-CoV-2 infection and transmission in the North American deer mouse. Nat Commun. 2021;12(1):3612. doi: 10.1038/s41467-021-23848-9. PMCID: PMC8203675.
34. Hall ER. Mammals of North America. New York, NY: John Wiley and Sons; 1979.
35. Hara I, Izui S, McConahey PJ, Elder JH, Jensen FC, Dixon FJ. Induction of high serum levels of retroviral env gene products (gp70) in mice by bacterial lipopolysaccharide. Proc Natl Acad Sci U S A. 1981;78(7):4397-401. doi: 10.1073/pnas.78.7.4397. PMCID: PMC319797.

36. Hart SN, Therneau TM, Zhang Y, Poland GA, Kocher JP. Calculating sample size estimates for RNA sequencing data. J Computational Biol. 2013;20(12):970-8. doi: 10.1089/cmb.2012.0283. PMCID: PMC3842884.
37. Hedges LV, Gurevitch J, Curtis PS. The meta-analysis of response ratios in experimental ecology. Ecology. 1999;80(4):1150-6. doi: 10.1890/11-0423.1.
38. Heinzelmann M, Polk Jr HC, Chernobelsky A, Stites TP, Gordon LE. Endotoxin and muramyl dipeptide modulate surface receptor expression on human mononuclear cells. Immunopharmacology. 2000;48(2):117-28. doi: 10.1016/s0162-3109(00)00195-8. PMID: 10936509.
39. Hilton HG, Rubinstein ND, Janki P, Ireland AT, Bernstein N, Fong NL, Wright KM, Smith M, Finkle D, Martin-McNulty B, Roy M, Imai DM, Jojic V, Buffenstein R. Single-cell transcriptomics of the naked mole-rat reveals unexpected features of mammalian immunity. PLoS Biol. 2019;17(11):e3000528. doi: 10.1371/journal.pbio.3000528. PMCID: PMC6894886.
40. Hoen AG, Margos G, Bent SJ, Diuk-Wasser MA, Barbour A, Kurtenbach K, Fish D. Phylogeography of Borrelia burgdorferi in the eastern United States reflects multiple independent Lyme disease emergence events. Proc Natl Acad Sci U S A. 2009;106(35):15013-8. doi: 10.1073/pnas.0903810106. PMCID: 2727481.
41. Hurst TP, Magiorkinis G. Activation of the innate immune response by endogenous retroviruses. J Gen Virol. 2015;96(Pt 6):1207-18. doi: 10.1099/jgv.0.000017. PubMed PMID: 26068187.
42. Italiani P, Boraschi D. From Monocytes to M1/M2 Macrophages: phenotypical vs. functional differentiation. Front Immunol. 2014;5:514. doi: 10.3389/fimmu.2014.00514. PMCID: PMC4201108.
43. Johnson TL, Fischer RJ, Raffel SJ, Schwan TG. Host associations and genomic diversity of Borrelia hermsii in an endemic focus of tick-borne relapsing fever in western North America. Parasit Vectors. 2016;9(1):575. Epub 2016/11/12. doi: 10.1186/s13071-016-1863-0. PMCID: PMC5105259.
44. Jongstra J, Moroni C. Lipopolysaccharide induces retroviral antigen expression in 129/J mouse lymphocytes: evidence for assembly of a defective viral particle. J Virol. 1981;37(3):1044-50. doi: 10.1128/jvi.37.3.1044-1050.1981. PMCID: PMC171101.
45. Joyner CP, Myrick LC, Crossland JP, Dawson WD. Deer mice as laboratory animals. ILAR. 1998;39(4):322-30. PubMed PMID: 11406688.
46. Kong L, Sun L, Zhang H, Liu Q, Liu Y, Qin L, Shi G, Hu JH, Xu A, Sun YP, Li D, Shi YF, Zang JW, Zhu J, Chen Z, Wang ZG, Ge BX. An essential role for RIG-I in toll-like receptor-stimulated phagocytosis. Cell host & microbe. 2009;6(2):150-61. doi: 10.1016/j.chom.2009.06.008. PubMed PMID: 19683681.
47. Kuroda E, Kito T, Yamashita U. Reduced expression of STAT4 and IFN-γ in macrophages from BALB/c mice. J Immunol. 2002;168(11):5477-82. doi: 10.4049/jimmunol.168.11.5477.
48. Labinskyy N, Mukhopadhyay P, Toth J, Szalai G, Veres M, Losonczy G, Pinto JT, Pacher P, Ballabh P, Podlutsky A, Austad SN, Csiszar A, Ungvari Z. Longevity is associated with increased vascular resistance to high glucose-induced oxidative stress and inflammatory gene expression in Peromyscus leucopus. Am J Physiol Heart Circ Physiol. 2009;296(4):H946-56. doi: 10.1152/ajpheart.00693.2008. PMCID: PMC2670687.
49. Langeroudi AG, Hirsch CM, Estabragh AS, Meinardi S, Blake DR, Barbour AG. Elevated carbon monoxide to carbon dioxide ratio in the exhaled breath of mice treated with a single dose of lipopolysaccharide. Open Forum Infect Dis. 2014;1(2):ofu085. doi: 10.1093/ofid/ofu085. PMCID: PMC4281777.
50. Levengood JM, Heske EJ. Heavy metal exposure, reproductive activity, and demographic patterns in white-footed mice (Peromyscus leucopus) inhabiting a contaminated floodplain wetland. Sci Total Environ. 2008;389(2-3):320-8. doi: 10.1016/j.scitotenv.2007.08.050. PMID: 17900661.

51. Lima-Junior DS, Krishnamurthy SR, Bouladoux N, Collins N, Han SJ, Chen EY, Constantinides MG, Link VM, Lim AI, Enamorado M, Cataisson C, Gil L, Rao I, Farley TK, Koroleva G, Attig J, Yuspa SH, Fischbach MA, Kassiotis G, Belkaid Y. Endogenous retroviruses promote homeostatic and inflammatory responses to the microbiota. Cell. 2021;184(14):3794-811.e19. doi: 10.1016/j.cell.2021.05.020. PMCID: PMC8381240.
52. Long A, Baldwin-Brown J, Tao Y, Cook V, Balderrama-Gutierrez G, Corbett-Detig R, Mortazavi A, Barbour A. The genome of Peromyscus leucopus, natural host for Lyme disease and other emerging infections. Sci Advances. 2019;5(7):eaaw6441. doi: 10.1126/sciadv.aaw6441; PMCID: PMC6656541.
53. Long PN, Cook VJ, Majumder A, Barbour AG, Long AD. The utility of a closed breeding colony of Peromyscus leucopus for dissecting complex traits. Genetics. 2022;221(1). doi: 10.1093/genetics/iyac026. PMCID: PMC9071557.
54. Loría-Cervera EN, Sosa-Bibiano EI, Van Wynsberghe NR, Andrade-Narváez FJ. Finding a model for the study of Leishmania (Leishmania) mexicana infection: the Yucatan Deer mouse (Peromyscus yucatanicus) as a suitable option. Acta Trop. 2018;187:158-64. doi: 10.1016/j.actatropica.2018.08.003. PubMed PMID: 30092224.
55. Lowenstein CJ, Alley EW, Raval P, Snowman AM, Snyder SH, Russell SW, Murphy WJ. Macrophage nitric oxide synthase gene: two upstream regions mediate induction by interferon gamma and lipopolysaccharide. Proc Natl Acad Sci U S A. 1993;90(20):9730-4. PMCID: PMC47644.
56. MacMicking JD, Nathan C, Hom G, Chartrain N, Fletcher DS, Trumbauer M, Stevens K, Xie Q-w, Sokol K, Hutchinson N, Chen H, Mudget JS. Altered responses to bacterial infection and endotoxic shock in mice lacking inducible nitric oxide synthase. Cell. 1995;81(4):641-50. doi: 10.1016/0092-8674(95)90085-3.
57. Mandl JN, Schneider C, Schneider DS, Baker ML. Going to bat(s) for studies of disease tolerance. Front Immunol. 2018;9:2112. doi: 10.3389/fimmu.2018.02112. PMCID: PMC6158362.
58. Mazgaeen L, Gurung P. Recent Advances in Lipopolysaccharide Recognition Systems. Int J Molec Sci. 2020;21(2). doi: 10.3390/ijms21020379. PMCID: PMC7013859.
59. McCarthy DJ, Chen Y, Smyth GK. Differential expression analysis of multifactor RNA-Seq experiments with respect to biological variation. Nucleic Acids Res. 2012;40(10):4288-97. doi: 10.1093/nar/gks042; PMCID: PMC3378882
60. McClure M, Kaye S. Can detection of xenotropic murine leukemia virus-related virus be linked to chronic fatigue syndrome? Expert Rev Molec Diagnostics. 2010;10(5):537-9.
61. Milovic A, Bassam K, Shao H, Chatzistamou I, Tufts DM, Diuk-Wasser M, Barbour AG. Lactobacilli and other gastrointestinal microbiota of Peromyscus leucopus, reservoir host for agents of Lyme disease and other zoonoses in North America. PLoS One. 2020;15(8):e0231801. doi: 10.1371/journal.pone.0231801. PMCID: PMC7446861.
62. Mlera L, Meade-White K, Saturday G, Scott D, Bloom ME. Modeling Powassan virus infection in Peromyscus leucopus, a natural host. PLoS Negl Trop Dis. 2017;11(1):e0005346. doi: 10.1371/journal.pntd.0005346. PMCID: PMC5302833.
63. Mommert M, Tabone O, Guichard A, Oriol G, Cerrato E, Denizot M, Cheynet V, Pachot A, Lepape A, Monneret G, Venet F, Brengel-Pesce K, Textoris J, Mallet F. Dynamic LTR retrotransposon transcriptome landscape in septic shock patients. Crit Care. 2020;24(1):96. doi: 10.1186/s13054-020-2788-8. PMCID: PMC7081582.
64. Moody KD, Terwilliger GA, Hansen GM, Barthold SW. Experimental Borrelia burgdorferi infection in Peromyscus leucopus. J Wildl Dis. 1994;30(2):155-61. doi: 10.7589/0090-3558-30.2.155. PubMed PMID: 8028098.
65. Morzunov SP, Rowe JE, Ksiazek TG, Peters CJ, St Jeor SC, Nichol ST. Genetic analysis of the diversity and origin of hantaviruses in Peromyscus leucopus mice in North America. J Virol. 1998;72(1):57-64. PMCID: PMC109349.

66. Moscarella RA, Hoffman SMG, Myers P, Yahnke CJ, Lundrigan BL. Genetic and demographic analysis of invasive Peromyscus leucopus in the northern Great Lakes region. J Mammal 2019;100(2):345-53. doi: 10.1093/jmammal/gyz053.
67. Munshi-South J, Kharchenko K. Rapid, pervasive genetic differentiation of urban white-footed mouse (Peromyscus leucopus) populations in New York City. Mol Ecol. 2010, doi: 10.1111/j.1365-294X.2010.04816.x. PubMed PMID: 20819163.
68. Murray PJ. Macrophage polarization. Ann Rev Physiol. 2017;79:541-66. doi: 10.1146/annurev-physiol-022516-034339
69. Murray PJ, Allen JE, Biswas SK, Fisher EA, Gilroy DW, Goerdt S, Gordon S, Hamilton JA, Ivashkiv LB, Lawrence T, Locati M, Mantovani A, Martinez FO, Mege JL, Mosser DM, Natoli G, Saeij JP, Schultze JL, Shirey KA, Sica A, Suttles J, Udalova I, van Ginderachter JA, Vogel SN, Wynn TA. Macrophage activation and polarization: nomenclature and experimental guidelines. Immunity. 2014;41(1):14-20. doi: 10.1016/j.immuni.2014.06.008. PMCID: PMC4123412.
70. Narasimhan PB, Marcovecchio P, Hamers AAJ, Hedrick CC. Nonclassical Monocytes in Health and Disease. Annu Rev Immunol. 2019;37:439-56. doi: 10.1146/annurev-immunol-042617-053119. PubMed PMID: 31026415.
71. Nathan C. Nonresolving inflammation redux. Immunity. 2022;55(4):592-605. doi: 10.1016/j.immuni.2022.03.016. PMCID: PMC9003810.
72. Norgard MV, Arndt LL, Akins DR, Curetty LL, Harrich DA, Radolf JD. Activation of human monocytic cells by Treponema pallidum and Borrelia burgdorferi lipoproteins and synthetic lipopeptides proceeds via a pathway distinct from that of lipopolysaccharide but involves the transcriptional activator NF-kappa B. Infect Immun. 1996;64(9):3845-52. doi: 10.1128/iai.64.9.3845-3852.1996. PMCID: PMC174301.
73. Oka K, Yamakawa M, Kawamura Y, Kutsukake N, Miura K. The Naked Mole-Rat as a model for healthy aging. Annu Rev Anim Biosci. 2023;11:207-26. doi: 10.1146/annurev-animal-050322-074744. PubMed PMID: 36318672.
74. Pisano MP, Tabone O, Bodinier M, Grandi N, Textoris J, Mallet F, Tramontano E. RNA-Seq transcriptome analysis reveals Long Terminal Repeat retrotransposon modulation in human peripheral blood mononuclear cells after in vivo lipopolysaccharide injection. J Virol. 2020;94(19). Epub 20200915. doi: 10.1128/jvi.00587-20. PubMed PMID: 32669333; PMCID: PMC7495373.
75. Quatrini L, Wieduwild E, Guia S, Bernat C, Glaichenhaus N, Vivier E, Ugolini S. Host resistance to endotoxic shock requires the neuroendocrine regulation of group 1 innate lymphoid cells. J Exp Med. 2017;214(12):3531-41. doi: 10.1084/jem.20171048. PMCID: PMC5716043.
76. Rangel SC, da Silva MD, da Silva AL, Dos Santos JMB, Neves LM, Pedrosa A, Rodrigues FM, Trettel CDS, Furtado GE, de Barros MP, Bachi ALL, Romano CM, Nali L. Human endogenous retroviruses and the inflammatory response: a vicious circle associated with health and illness. Front Immunol. 2022;13:1057791. doi: 10.3389/fimmu.2022.1057791. PMCID: PMC9744114.
77. Robinson MD, Oshlack A. A scaling normalization method for differential expression analysis of RNA-seq data. Genome Biol. 2010;11(3):R25. doi: 10.1186/gb-2010-11-3-r25. PMCID: PMC2864565.
78. Russ E, Iordanskiy S. Endogenous retroviruses as modulators of innate immunity. Pathogens. 2023;12(2):162. doi: 10.3390/pathogens12020162. PMCID: PMC9963469
79. Sacher GA, Hart RW. Longevity, aging and comparative cellular and molecular biology of the house mouse, Mus musculus, and the white-footed mouse, Peromyscus leucopus. Birth Defects Orig Artic Ser. 1978;14(1):71-96. PubMed PMID: 343832.
80. Salazar JC, Duhnam-Ems S, La Vake C, Cruz AR, Moore MW, Caimano MJ, Velez-Climent L, Shupe J, Krueger W, Radolf JD. Activation of human monocytes by live Borrelia burgdorferi generates TLR2-dependent and -independent responses which include induction of IFN-beta. PLoS Pathogens. 2009;5(5):e1000444. doi: 10.1371/journal.ppat.1000444. PMCID: PMC2679197.

81. Salkowski CA, Detore G, McNally R, van Rooijen N, Vogel SN. Regulation of inducible nitric oxide synthase messenger RNA expression and nitric oxide production by lipopolysaccharide in vivo: the roles of macrophages, endogenous IFN-gamma, and TNF receptor-1-mediated signaling. J Immunol. 1997;158(2):905-12. PubMed PMID: 8993010.
82. Schnizlein-Bick CT, Mandy FF, O'Gorman MR, Paxton H, Nicholson JK, Hultin LE, Gelman RS, Wilkening CL, Livnat D. Use of CD45 gating in three and four-color flow cytometric immunophenotyping: guideline from the National Institute of Allergy and Infectious Diseases, Division of AIDS. Cytometry. 2002;50(2):46-52. doi: 10.1002/cyto.10073. PubMed PMID: 12116345.
83. Schwanz LE, Voordouw MJ, Brisson D, Ostfeld RS. Borrelia burgdorferi has minimal impact on the Lyme disease reservoir host Peromyscus leucopus. Vector Borne Zoonotic Dis. 2011;11(2):117-24. doi: 10.1089/vbz.2009.0215. PubMed PMID: 20569016.
84. Soudi S, Zavaran-Hosseini A, Muhammad Hassan Z, Soleimani M, Jamshidi Adegani F, Hashemi SM. Comparative study of the effect of LPS on the function of BALB/c and C57BL/6 peritoneal macrophages. Cell Journal (Yakhteh). 2013;15(1):45-54.
85. Steere AC, Bartenhagen NH, Craft JE, Hutchinson GJ, Newman JH, Pachner AR, Rahn DW, Sigal LH, Taylor E, Malawista SE. Clinical manifestations of Lyme disease. Zentralbl Bakteriol Mikrobiol Hyg [A]. 1986;263(1-2):201-5.
86. Steere AC, Sikand VK, Meurice F, Parenti DL, Fikrig E, Schoen RT, Nowakowski J, Schmid CH, Laukamp S, Buscarino C, Krause DS. Vaccination against Lyme disease with recombinant Borrelia burgdorferi outer-surface lipoprotein A with adjuvant. Lyme Disease Vaccine Study Group. N Engl J Med. 1998;339(4):209-15. doi: 10.1056/NEJM199807233390401.
87. Stoye JP, Moroni C. Endogenous retrovirus expression in stimulated murine lymphocytes. Identification of a new locus controlling mitogen induction of a defective virus. J Exp Med. 1983;157(5):1660-74. doi: 10.1084/jem.157.5.1660. PMCID: PMC2187009.
88. Takayama K, Rothenberg RJ, Barbour AG. Absence of lipopolysaccharide in the Lyme disease spirochete, Borrelia burgdorferi. Infect Immun. 1987;55(9):2311-3. doi: 10.1128/iai.55.9.2311-2313.1987. PMCID: PMC260699.
89. Treger RS, Pope SD, Kong Y, Tokuyama M, Taura M, Iwasaki A. The Lupus susceptibility locus Sgp3 encodes the Suppressor of Endogenous Retrovirus Expression SNERV. Immunity. 2019;50(2):334-47.e9. doi: 10.1016/j.immuni.2018.12.022. PMCID: PMC6382577.
90. van Stijn CM, Kim J, Lusis AJ, Barish GD, Tangirala RK. Macrophage polarization phenotype regulates adiponectin receptor expression and adiponectin anti-inflammatory response. FASEB J. 2015;29(2):636-49. doi: 10.1096/fj.14-253831. PMCID: PMC4314235.
91. Vergadi E, Ieronymaki E, Lyroni K, Vaporidi K, Tsatsanis C. Akt signaling pathway in macrophage activation and M1/M2 polarization. J Immunol. 2017;198(3):1006-14.
92. Voordouw MJ, Lachish S, Dolan MC. The Lyme disease pathogen has no effect on the survival of its rodent reservoir host. PLoS One. 2015;10(2):e0118265. doi: 10.1371/journal.pone.0118265. PMCID: PMC4331372.
93. Wei XQ, Charles IG, Smith A, Ure J, Feng GJ, Huang FP, Xu D, Muller W, Moncada S, Liew FY. Altered immune responses in mice lacking inducible nitric oxide synthase. Nature. 1995;375(6530):408-11. doi: 10.1038/375408a0. PubMed PMID: 7539113.
94. Wiedmeyer CE, Crossland JP, Veres M, Dewey MJ, Felder MR, Barlow SC, Vrana PB, Szalai G. Hematologic and serum biochemical values of 4 species of Peromyscus mice and their hybrids. JAALAS. 2014;53(4):336-43. PMCID: PMC4113232.
95. Wolf G, Yang P, Füchtbauer AC, Füchtbauer EM, Silva AM, Park C, Wu W, Nielsen AL, Pedersen FS, Macfarlan TS. The KRAB zinc finger protein ZFP809 is required to initiate epigenetic silencing of endogenous retroviruses. Genes Devel. 2015;29(5):538-54. doi: 10.1101/gad.252767.114. PMCID: PMC4358406.
96. Xiao W, Mindrinos MN, Seok J, Cuschieri J, Cuenca AG, Gao H, Hayden DL, Hennessy L, Moore EE, Minei JP, Bankey PE, Johnson JL, Sperry J, Nathens AB, Billiar TR, West MA,

Brownstein BH, Mason PH, Baker HV, Finnerty CC, Jeschke MG, López MC, Klein MB, Gamelli RL, Gibran NS, Arnoldo B, Xu W, Zhang Y, Calvano SE, McDonald-Smith GP, Schoenfeld DA, Storey JD, Cobb JP, Warren HS, Moldawer LL, Herndon DN, Lowry SF, Maier RV, Davis RW, Tompkins RG. A genomic storm in critically injured humans. J Exp Med. 2011;208(13):2581-90. doi: 10.1084/jem.20111354. PMCID: PMC3244029.

97. Yang P, Wang Y, Macfarlan TS. The role of KRAB-ZFPs in transposable element repression and mammalian evolution. Trends Genet. 2017;33(11):871-81. doi: 10.1016/j.tig.2017.08.006. PMCID: PMC5659910.
98. Zar JH. Biostatistical Analysis. 4th ed. Upper Saddle River, NJ, USA: Prentice Hall; 1999.
99. Zhou Y, Zhou B, Pache L, Chang M, Khodabakhshi AH, Tanaseichuk O, Benner C, Chanda SK. Metascape provides a biologist-oriented resource for the analysis of systems-level datasets. Nat Commun. 2019;10(1):1523. doi: 10.1038/s41467-019-09234-6. PMCID: PMC6447622.